

## States in $^{184}\text{W}$ via neutron capture and beta-decay excitations

D. L. Bushnell, J. Hawkins, and R. Goebbert

*Physics Department, Northern Illinois University, DeKalb, Illinois 60115*

R. K. Smither

*Physics Division, Argonne National Laboratory, Argonne, Illinois 60439*

(Received 6 March 1974; revised manuscript received 11 November 1974)

Thermal neutron capture and average resonance neutron capture in  $^{183}\text{W}$  yield two different  $\gamma$ -ray spectra made up of high energy primary transitions from the capture state to low-lying levels in  $^{184}\text{W}$ . These spectra along with medium energy spectra following thermal capture and  $\gamma$ - $\gamma$  coincidence spectra produced from  $\beta$  decay of  $^{184}\text{Re}$  provides the basis for the study of 43 states in  $^{184}\text{W}$  ranging in energy up to 2404 keV. A level scheme has been constructed that incorporates 50  $\gamma$  rays having energies ranging from 600 to 2400 keV. Five energy levels not previously reported in the literature have been discovered and  $J^\pi$  assignments for over six other levels have been improved so that parities are certain in most cases while spin choices are narrowed to at most two. All positive parity states below 2404 keV having spins 0, 1, or 2 have been detected and most if not all have been given a definitive positive parity assignment. In addition, many negative parity states having low spin values have been identified. Disagreements with  $J^\pi$  assignments previously reported in the literature are discussed.

NUCLEAR STRUCTURE  $^{183}\text{W}(n, \gamma)$   $E_\gamma=607$  keV–2690 keV.  $^{183}\text{W}(\bar{n}, \gamma)$   $E_\gamma=5008$  keV–7412 keV, Ge(Li) detector; deduced  $^{184}\text{W}$  levels,  $J, \pi$ .  $^{184}\text{Re}$ ,  $^{184}\text{Re}^m$   $\beta$ ,  $\gamma\gamma$ -coin,  $^{184}\text{W}$  levels.

### INTRODUCTION

Past research on the characteristics of nuclear states in  $^{184}\text{W}$  have employed  $\beta$ -decay excitation,<sup>1-8</sup> thermal neutron capture,<sup>9-11</sup> resonance neutron capture,<sup>12-16</sup> and average capture with 2 keV neutrons.<sup>11</sup> The resulting information provides a valuable basis for constructing partial level schemes for  $^{184}\text{W}$  up to about 2.5 MeV. In addition inelastic deuteron scattering,<sup>17</sup> Coulomb excitation,<sup>18,19</sup> and neutron transfer reactions<sup>20,21</sup> have been employed to produce and describe collective excitations and two-quasiparticle states in the isotopes of tungsten. Special features such as parity impurities and the measurement of transition multipolarities have been studied using oriented nuclei.<sup>22-24</sup>

By employing techniques of neutron capture  $\gamma$ -ray spectroscopy, valuable information about levels whose energies are greater than the energy difference corresponding to the ground state mass difference between  $^{184}\text{Re}$  and  $^{184}\text{W}$  (~1600 keV) can be obtained. Below this energy the results of  $(n, \gamma)$  studies help to provide spin and parity assignments and precision energies for most levels excited by  $\beta$  decay, thus allowing the comparison of results of independent measurements.

The so-called average resonance neutron capture method for producing neutron capture  $\gamma$ -ray

spectra developed by Bollinger and Thomas<sup>25</sup> lends itself to the study of low-lying nuclear states. We have made use of this technique to locate the low spin positive parity states in  $^{184}\text{W}$  up to 2404 keV and many of the low spin negative parity states. Thermal neutron capture is used to provide primary transitions for comparison with those from the average capture and also to produce transitions between the low-lying states. We have also made radioactive decay studies employing  $\gamma$ - $\gamma$  coincidence spectroscopy to give us a first hand account describing states up to the  $\beta$  excitation limit at about 1500 keV.

### $\beta$ -DECAY AND $\gamma$ - $\gamma$ COINCIDENCE SPECTRA

Levels in  $^{184}\text{W}$  are excited by electron capture from the ground state ( $T=38$  days) and from an isomeric state ( $T=169$  days) of  $^{184}\text{Re}$ .  $\gamma$ -ray transitions among the  $^{184}\text{W}$  levels were studied using a  $\gamma$ - $\gamma$  coincidence spectrometer.

Several methods of producing the  $^{184}\text{Re}$  activity were used. An  $(\alpha, n)$  reaction on  $^{181}\text{Ta}$  accomplished in the Argonne National Laboratory 60 inch cyclotron produced the desired activity, but troublesome amounts of activity from  $^{182}\text{Ta}$  and  $^{183}\text{Re}$  existed in the sample also. In order to avoid expensive chemical separations, we tried the  $^{185}\text{Re}(\gamma, n)^{184}\text{Re}$  reaction on a natural abundance

TABLE I. Standard  $\gamma$ -ray energies used for the energy calibration and determination of the system linearity of the  $\gamma$ - $\gamma$  coincidence spectrometer.

Radio nuclide	$\gamma$ -ray energy (keV)	Reference
$^{133}\text{Ba}$	$80.998 \pm 0.008$	a
$^{57}\text{Co}$	$121.97 \pm 0.05$	b
$^{57}\text{Co}$	$136.33 \pm 0.04$	b
$^{133}\text{Ba}$	$276.397 \pm 0.012$	a
$^{133}\text{Ba}$	$302.851 \pm 0.015$	a
$^{133}\text{Ba}$	$356.055 \pm 0.017$	a
$^{133}\text{Ba}$	$383.851 \pm 0.020$	a
$^{22}\text{Na}$	$511.006 \pm 0.003$	c
$^{137}\text{Cs}$	$661.595 \pm 0.076$	d
$^{46}\text{Sc}$	$889.18 \pm 0.10$	e
$^{46}\text{Sc}$	$1120.41 \pm 0.10$	e
$^{60}\text{Co}$	$1173.26 \pm 0.05$	f
$^{22}\text{Na}$	$1274.55 \pm 0.04$	c
$^{60}\text{Co}$	$1332.48 \pm 0.05$	f

<sup>a</sup> R. C. Greenwood, R. G. Helmer, and R. J. Gehrke, Nucl. Instrum. Methods **77**, 141 (1970).

<sup>b</sup> J. B. Marion, University of Maryland Technical Report 16, 653, 1957 (unpublished).

<sup>c</sup> Nucl. Data **A4**, (1968).

<sup>d</sup> R. L. Graham, G. T. Ewan, and J. S. Geiger, Nucl. Instrum. Methods **9**, 245 (1960).

<sup>e</sup> J. J. Reidy and M. L. Wiedenbeck, Nucl. Phys. **70**, 518 (1965).

<sup>f</sup> R. E. Berg and E. Kashy, Nucl. Instrum. Methods **39**, 169 (1966).

rhodium sample employing the electron linac at Argonne National Laboratory. We are able to avoid the necessity of chemical separations since the two unwanted activities from  $^{186}\text{Re}$  and  $^{183}\text{Re}$  were not produced in sufficient quantities to interfere in the analysis of the spectrum. In the former case, an initially strong activity of 90 h half-life conveniently died out relative to the 38-day and 169-day activities of  $^{184}\text{Re}$ .  $\gamma$  rays associated with the initially very weak  $^{183}\text{Re}$  activity were not close in energy to the  $\gamma$ -ray energies used for gates in the coincidence measurements on  $^{184}\text{W}$ . Though its activity grew relative to the 38-day lines, half-life measurements provided distinct labels for identification and, even after several months of coincidence measurements, no difficulty arose from this  $^{183}\text{Re}$  contamination.

The  $20\text{ cm}^3$  Ge(Li) detector used in this experiment has an efficiency of 3.0% compared to NaI(Tl) at 1332 keV and was calibrated using the standard lines listed in Table I. Table II lists the results obtained from a singles spectra such as the one shown in Fig. 1. The change in the relative strengths of the lines as seen in columns 2 and 3 is due to the fact that two  $^{184}\text{Re}$  parent states having half-lives of 38 and 169 days feed levels

TABLE II.  $\gamma$ -ray energies and relative intensities (normalized to 100 for the 903.4 keV  $\gamma$ -ray) for the  $\beta$  decay of  $^{184}\text{Re}$  to  $^{184}\text{W}$ . Columns 2 and 3 list these intensities ( $I_r$ ) corresponding respectively to 44 and 119 days after the source activity was made. The energy uncertainties are in keV and are based on a combination of statistical and calibration uncertainties. The intensity uncertainties are in %. A square bracket around a  $\gamma$ -ray energy means that it was observed in coincidence data only and the corresponding intensity has been calculated relative to the 119 day data.  $\gamma$  rays marked with an asterisk arise predominantly from the metastable state of  $^{184}\text{Re}$ .

$\gamma$ -ray energy (keV)	Intensity $I_r \pm \frac{\Delta I_r \times 100}{I_r}$ (After 44 days)	Intensity $I_r \pm \frac{\Delta I_r \times 100}{I_r}$ (After 119 days)	Initial state in $^{184}\text{W}$ (keV)
$111.24 \pm 0.06$	$12.5 \pm 6$	$18.7 \pm 5$	111.24
$216.0 \pm 0.5^*$	$0.24 \pm 9$	$0.47 \pm 7$	1221.7, 1501.1
$226.1 \pm 0.4$	$0.08 \pm 16$	$0.08 \pm 29$	1129.1
$252.84 \pm 0.05$	$8.71 \pm 10$	$7.75 \pm 5$	364.08
$318.2 \pm 0.1^*$	$0.13 \pm 13$	$0.34 \pm 15$	1221.7
$384.0 \pm 0.3^*$	$0.08 \pm 28$	$0.21 \pm 8$	748.1
[482.4 $\pm$ 0.3]	...	$0.06 \pm 26$	1386.5
$536.2 \pm 0.6^*$	$0.05 \pm 30$	$0.15 \pm 27$	1285.1
$539.2 \pm 0.2$	$0.83 \pm 12$	$0.89 \pm 14$	903.3
$641.9 \pm 0.1$	$5.24 \pm 11$	$5.05 \pm 10$	1005.9
$756.5 \pm 0.4$	$0.17 \pm 17$	$0.17 \pm 17$	1121.5
$769.8 \pm 0.2$	$1.88 \pm 11$	$1.38 \pm 11$	1133.8
$792.1 \pm 0.1$	$102 \pm 11$	$97.0 \pm 10$	903.3
$894.8 \pm 0.2$	$40.3 \pm 11$	$43.3 \pm 10$	1005.9
$903.4 \pm 0.2$	$100.00 \pm 11$	$100.00 \pm 10$	903.3
$921.1 \pm 0.2^*$	$0.15 \pm 12$	$0.48 \pm 10$	1285.1
$1010.3 \pm 0.7$	$0.23 \pm 11$	$0.24 \pm 12$	1121.5
[1017.5 $\pm$ 0.7]	...	$0.04 \pm 29$	1129.1(dash)
$1022.4 \pm 0.4$	$1.38 \pm 10$	$1.40 \pm 10$	1133.8
$1110.3 \pm 0.5^*$	$0.01 \pm 46$	$0.03 \pm 15$	1221.7
$1121.1 \pm 0.4$	$0.09 \pm 13$	$0.15 \pm 11$	1121.5
$1173.8 \pm 0.4^*$	$0.02 \pm 32$	$0.05 \pm 32$	1285.1
$1275.3 \pm 0.2$	$0.28 \pm 11$	$0.30 \pm 11$	1386.5
$1314.4 \pm 0.4$	$0.03 \pm 15$	$0.03 \pm 16$	1314.4(dash)
$1386.5 \pm 0.2$	$0.24 \pm 12$	$0.27 \pm 12$	1386.5
$1430.5 \pm 0.6$	$0.006 \pm 51$	$0.009 \pm 50$	1430.5(dash)

in  $^{184}\text{W}$ . This serves as an aid to determining which  $\gamma$  rays have the same initial state. In Table III we list the results of the analyses of gated spectra and in Fig. 2 we present two examples of these coincidence spectra.

The level scheme deduced from this data is presented in Fig. 3. This level scheme is substantially the same as that reported by Kukoc *et al.*<sup>4</sup> except for the level which we observe at 1431 keV. There is supporting evidence from our  $(n, \gamma)$  results for a positive parity low spin state at this energy. This leaves a puzzle as to where to place the 1314 keV  $\gamma$  ray. If we choose to include a level of this energy, it should be low spin in order to decay to the

ground state. However, the neutron capture  $\gamma$ -ray results (described later) do not suggest a low spin state at this energy. Placing it at the first excited state (as first suggested by Kukoc *et al.*<sup>4</sup>) predicts a level at 1426 keV but we have no  $(n, \gamma)$  support for this level either. However, the spin may be too high to be fed by primaries from the  $(n, \gamma)$  reaction. Placement at a higher excited state would require an energy greater than the ground state rest mass differences between  $^{184}\text{Re}$  and  $^{184}\text{W}$  and a level not observed in  $(n, \gamma)$  spectroscopy. As will be discussed later, a 1431.5 keV  $\gamma$  ray observed in the medium energy  $(n, \gamma)$  spectrum is interpreted to be a transition to the ground state from a level at 1431.5 keV. The recent  $\beta$  decay studies of McMillan *et al.*<sup>8</sup> suggests both a 1431 keV  $2^+$  state and a 1425 keV  $3^+$  state. The latter state is suggested also by Yates *et al.*<sup>7</sup> from the 8.7 h decay of  $^{184}\text{Ta}$ , by Kleinheinz, Daly, and Casten<sup>20</sup> using the  $^{183}\text{W}(d, p)$  reaction and by Casten and Kane<sup>16</sup> using resonance neutron capture. The 1431 keV state, though not reported by the other  $\beta$ -decay studies, is supported by Coulomb excitation,<sup>17</sup> resonance neutron capture,<sup>15,16</sup> and by the  $(n, \gamma)$  work of Greenwood and Reich.<sup>11</sup> We failed to ob-

serve the  $6^-$  state at 1446 keV reported in Ref. 6, 7, and 8 based on  $\beta$ -decay excitation and in Ref. 20 based on the  $(d, p)$  reaction, which is probably due to the lack of sufficient sensitivity in our  $\beta$ -decay spectra.

Our  $\gamma$ - $\gamma$  coincidence results require the placement of 3  $\gamma$  transitions (1173.8, 921.1, and 536.2 keV) at a level energy of  $1285.1 \pm 0.6$  keV. As can be seen by reference to Table II, each of these transitions exhibit the longer half-life associated with the metastable state of  $^{184}\text{Re}$ . Various authors<sup>2-4</sup> have made a spin and parity assignment of  $5^-$  to this state and recently Krane, Olsen, and Steyert<sup>24</sup> have examined the possibility of parity impurity to explain the 1173.8 keV transition. This level will be discussed later in the light of conclusions based on average resonance neutron capture spectra.

#### NEUTRON CAPTURE $\gamma$ -RAY SPECTRA

We have examined  $\gamma$ -ray transitions following neutron capture in  $^{183}\text{W}$  by use of a Compton suppression pair spectrometer,<sup>26</sup> which is located at a through hole of the CP-5 research reactor at

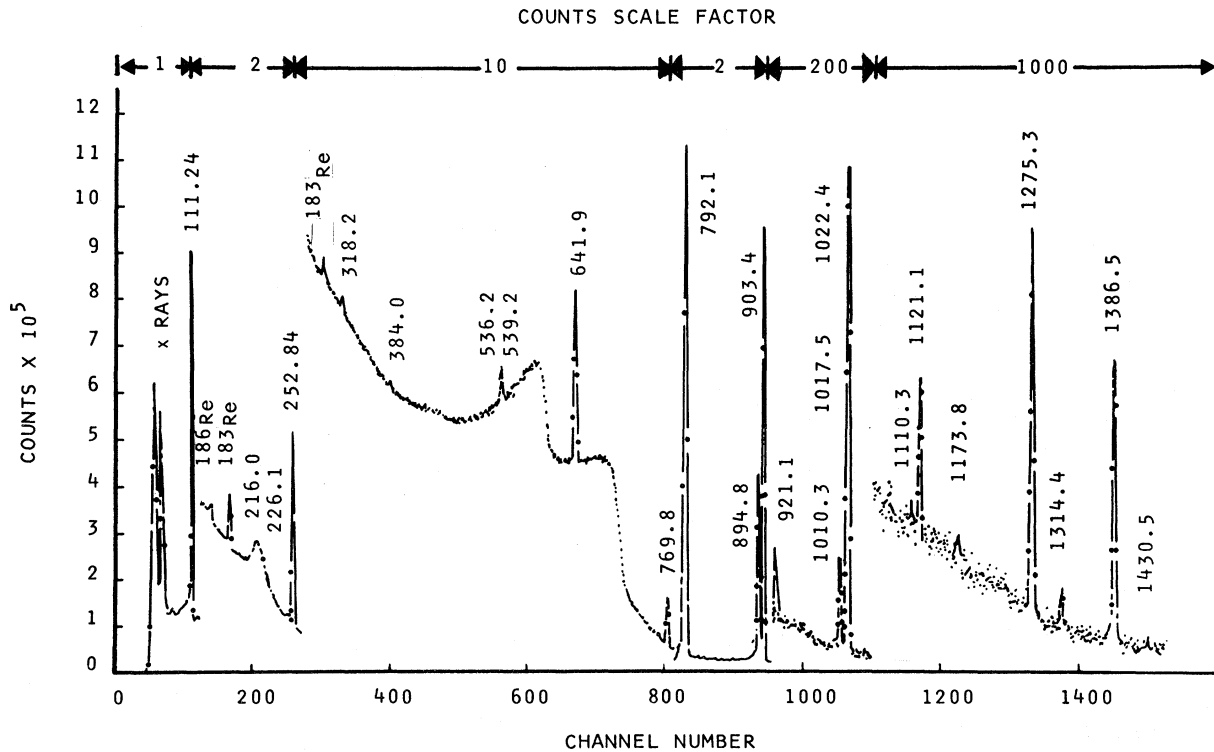


FIG. 1. A singles spectrum for the  $^{184}\text{Re}$  source. A scale factor inserted in each section of the figure represents the vertical magnification relative to the first section. The peaks at 1110.3, 1173.8, and 1430.5 keV were brought out more clearly in other singles runs while the lines at 216.0, 218.2, 384.0, and 482.4 keV were brought up more clearly in various coincidence spectra.

TABLE III.  $\gamma$ -ray counting rates observed for each of five coincidence gates.

$\gamma$ -ray energy (keV)	Coincidence gate position (keV)				
	111 keV+ x rays <sup>a</sup>	111	253	770-792 <sup>a</sup>	894-903
111.24	12220	975	7125	7365	10430
216.0			110		555
226.1			50	55	200
252.84	10800	3490	1705 <sup>b</sup>	3220 <sup>c</sup>	1930
318.2			45	115	540
384.0	195	70	320		
482.4				12	60
536.2 <sup>d</sup>					
539.2	580	215	1110		
641.9	2410	875	4930	35 <sup>b</sup>	90 <sup>b</sup>
756.5			110		
769.8	640	255	1680		
792.1	25750	11415	290 <sup>b</sup>	680 <sup>b</sup>	1070 <sup>b</sup>
894.8	9090	4010	80 <sup>b</sup>	250 <sup>b</sup>	420 <sup>b</sup>
903.4 <sup>e</sup>	10390 <sup>b</sup>	105 <sup>b</sup>	210 <sup>b</sup>	550 <sup>b</sup>	910 <sup>b</sup>
921.1	115	50	295		
1010.8	50	20			
1017.5 <sup>d</sup>					
1022.4	265	105	7		
1110.3 <sup>d</sup>					
1121.1 <sup>e</sup>					
1173.8	12	6			
1275.3	35	13			
1314.4 <sup>d</sup>					
1386.5 <sup>e</sup>					
1430.5 <sup>e</sup>					

<sup>a</sup> The data for these runs do not include random coincidence subtraction.

<sup>b</sup> These count rates are due to accidental coincidences.

<sup>c</sup> This count rate is a mixture of true coincidence counts from the 770 keV  $\gamma$  ray in the coincidence gate plus accidental coincidences of the 792.1 keV  $\gamma$  ray.

<sup>d</sup> Statistics in coincidence runs are not sufficient to detect the existence of these  $\gamma$  rays.

<sup>e</sup> These  $\gamma$  rays represent transitions to the ground state.

Argonne National Laboratory. This system employs a Ge(Li) detector having a volume of approximately 4 cm<sup>3</sup>, which is located on the axis and at the center of a large four-quadrant NaI(Tl) scintillation crystal. Associated with this spectrometer is an in-pile facility used to place targets in high neutron flux regions close to the reactor core.

Three somewhat different experimental arrangements were employed. First, spectra were taken of the high energy primary  $\gamma$ -ray transitions following thermal neutron capture in the target. About 180 mg of tungsten oxide powder were placed in a small graphite holder and positioned near the center of a through hole which passes through the high flux region on the reactor tangent to the reactor core. The spectrometer is operated in an electronic coincidence mode that rejects all pulses ex-

cept those associated with a pair production event in the Ge(Li) detector that leads to the escape of a pair of annihilation quanta, i.e. double escape.

A second kind of  $\gamma$ -ray spectrum containing energies from about 500 to 2500 keV was obtained using the same target as above located in a similar position. Full energy peaks were selected in this case by operating the spectrometer in the anticoincidence mode. In this mode the spectrum gate is closed whenever a quantum escapes from the Ge(Li) detector and is captured in a NaI(Tl) quadrant. These  $\gamma$  rays are envisioned to be associated with transitions in the lower energy regions of the level scheme and therefore capable of yielding information concerning the level structure of the nucleus in the lower region.

We have employed a third type of capture  $\gamma$ -ray experiment, referred to before as the average resonance neutron capture  $\gamma$ -ray method, in order to observe primary transitions to low-lying states following neutron capture in many resonances of the capture cross section. Since this process has been thoroughly discussed by Bollinger and Thomas,<sup>25</sup> we will provide only a brief general description here.

The  $\gamma$ -ray spectrum following neutron capture in a specific resonance of the capture cross section has an intensity pattern unique to that resonance. If the spectra from many resonances are superposed, the resulting spectrum will normally contain averaged intensities where transitions of the same multipolarity have about the same line strength. Thus *E1* transitions all have about the same intensity with variations consistent with the Porter-Thomas distribution. Such a spectrum can be obtained directly by use of the neutron flux of a reactor and a target surrounded by boron. The high intensity thermal part of the flux is removed, leaving a rather broad epithermal flux whose width covers many resonances of the neutron cross section.

The targets used to obtain the three kinds of spectra are all oxides of tungsten, and the isotopic abundances of the tungsten in these targets are listed in Table IV. In this table we use the notation that  $(\bar{n}, \gamma)$  means an average resonance neutron capture  $\gamma$ -ray reaction and that  $(n, \gamma)$  signifies a thermal neutron capture  $\gamma$ -ray reaction. We made use of a 0.5 g natural abundance metal tungsten target to obtain spectra used to assist in the identification of spectral lines not belonging to <sup>184</sup>W which appear in the  $(n, \gamma)$  spectra obtained using a target whose <sup>183</sup>W abundance is 82.5% (column 4, Table IV).

The mass of the enriched sample used for the <sup>183</sup>W( $\bar{n}, \gamma$ )<sup>183</sup>W reaction (column 3 of Table IV) is about 5 g, whereas the mass in the thermal cap-

ture case is only about 180 mg. This large difference in target mass occurs because of the need to at least partially restore some of the reaction rate which is lost due to the boron absorption employed to shift the energy centroid of the neutron flux out of the thermal region into the resonance region of the reaction cross section.

Isotopic identification of lines from the  $^{183}\text{W}(\bar{n},\gamma)-^{184}\text{W}$  reaction has been achieved primarily by comparing the resulting spectrum with a spectrum based on a natural abundance tungsten target which was provided to the authors by Thomas<sup>27</sup> at Argonne National Laboratory. Additional information for isotopic identification comes from comparing thermal and average resonance spectra.

In order to examine with sufficient detail those

primary transitions whose energies range from about 5000 to 7400 keV, two spectra having smaller but partially overlapping energy ranges were obtained. In order to facilitate isotopic identification of lines in the thermal capture spectra, the natural abundance runs were conducted with the same spectral energy ranges so that plots of both types of data when laid above and below each other readily revealed impurity lines. The results of these neutron capture  $\gamma$ -ray measurements will be discussed in detail later.

#### PRIMARY TRANSITIONS FROM THERMAL CAPTURE

Thermal neutron capture in  $^{183}\text{W}$  was carried out by placing a 180 mg enriched tungsten oxide sample inside a small carbon holder which is then

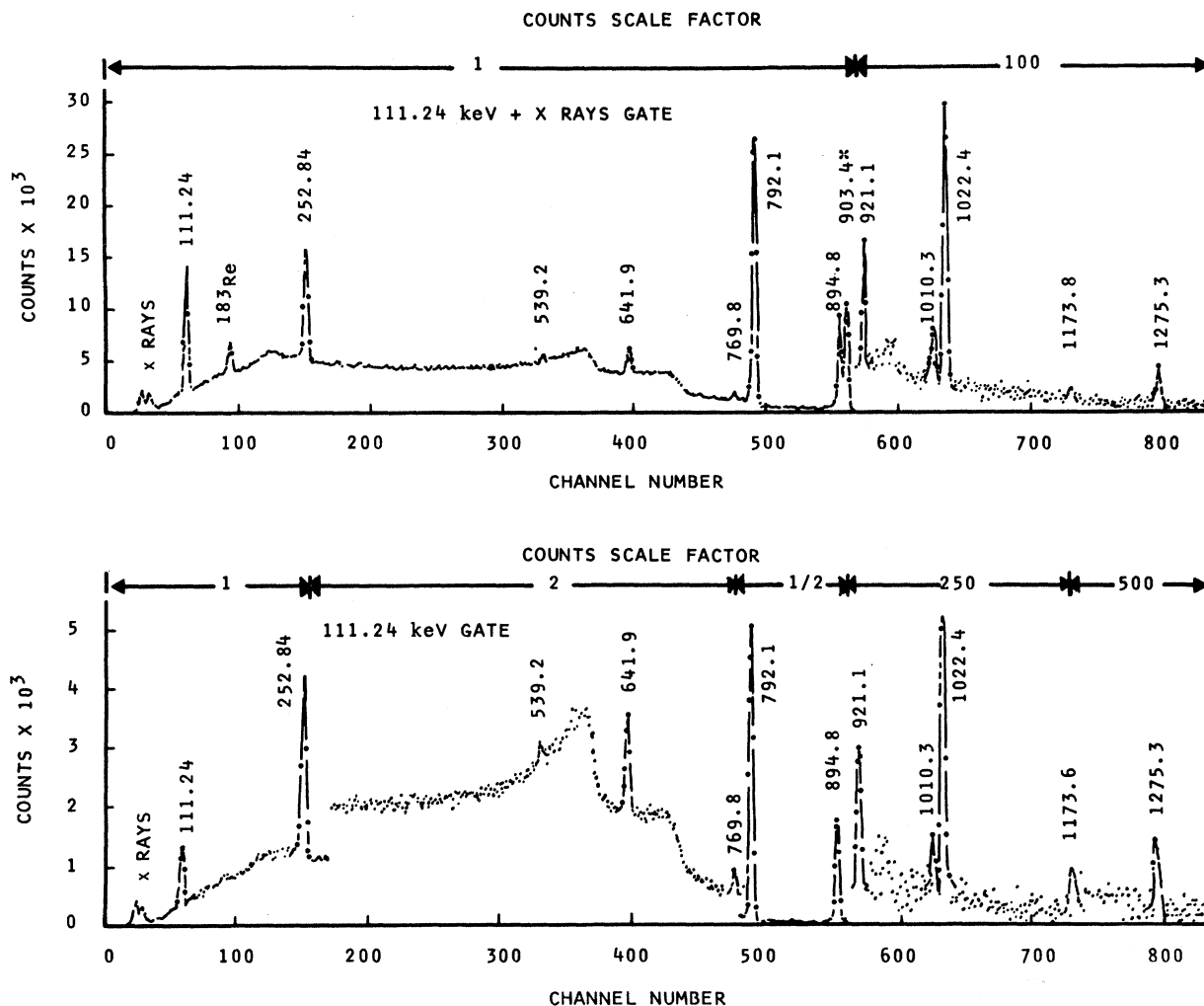


FIG. 2. Two examples of coincidence spectra taken with energy gates set in the NaI(Tl) counting arm. Random coincidence subtraction has been done for the shorter run time (26 h) case but not the other. An asterisk marks a line resulting from accidental coincidence.

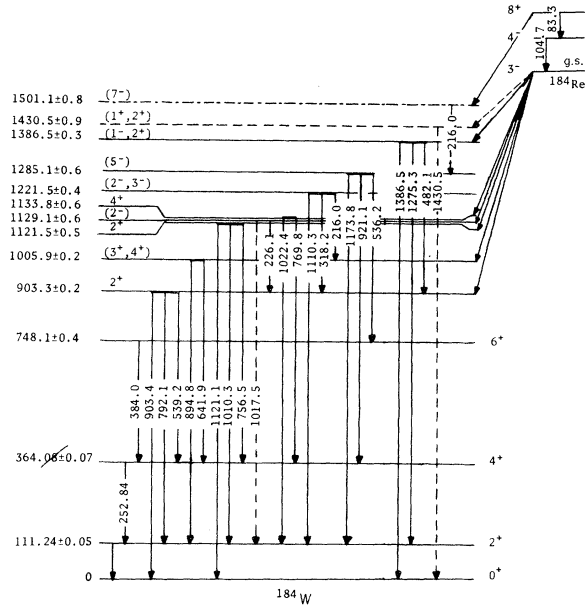


FIG. 3. Level scheme of  $^{184}\text{W}$  based on  $\gamma$ -ray spectroscopy following electron capture decay of  $^{184}\text{Re}$ . A square bracket around a  $J^\pi$  assignment means that it is based on our  $\beta$ -decay data and previously published results. The  $(2^-)$  at 1129.1 keV is a tentative spin assignment with definite parity as deduced from our  $(n, \gamma)$  work and the work of other authors (Refs. 6-8).

located in an intense thermal neutron flux. The isotopic abundance of this enriched sample is listed in column 4 of Table IV. A glance at column 5 of this table indicates that there is a predominance of thermal capture in  $^{183}\text{W}$ . This particular sample had previously been slightly contaminated with boron, having been used in a borated carbon sample holder; thus the standard spectral lines from the  $^{10}\text{B}(n, \gamma)^{11}\text{B}$  reaction appeared in the spectrum. These lines (6739.0 and 7006.3 keV)<sup>26,27</sup> do not interfere with any of the  $^{184}\text{W}$  lines and are used in the calibration along with lines from the  $^{14}\text{N}(n, \gamma)^{15}\text{N}$  reaction having energies 5269.2, 5533.2, and 6322.0 keV as reported by Thomas, Blatchley, and Bollinger<sup>26</sup> and later revised by Thomas<sup>27</sup> (see Table V).

Two spectra of primary lines representing partially overlapping  $\gamma$ -ray energy ranges (5.8 to 7.5 MeV and 4.6 to 6.4 MeV) from the  $^{183}\text{W}(n, \gamma)^{184}\text{W}$  reaction have been obtained using the coincidence mode of the Compton suppression pair spectrometer system.<sup>26</sup> In the cases where many days of data collection were needed, the spectrum in the multichannel analyzer was recorded and erased each day. The individual 1-day runs were then added together by a computer after eliminating any runs that showed signs of electronic drift. Typically, this resulted in a total of three to four

TABLE IV. Tungsten isotopic abundances in the tungsten oxide targets used for both thermal and average resonance neutron capture in  $^{183}\text{W}$  and in natural abundance tungsten. Thermal capture and average resonance capture are referred to as  $(n, \gamma)$  and  $(\bar{n}, \gamma)$ , respectively. Yields in terms of the number of thermal neutrons captured in an isotope for each 100 neutrons captured in all isotopes (%) are listed in columns 5 and 7 corresponding, respectively, to targets whose abundances are listed in columns 4 and 6.

$A$	$\sigma_{\text{thermal}}$ (b)	Enriched	Enriched	Yield (% of captures)	Natural	Yield (% of captures)
		$(\bar{n}, \gamma)$ (%)	$(n, \gamma)$ (%)		$(n, \gamma)$ (%)	
180	~10	<0.1	<0.1		0.14	1.4
182	20.5	5.4	6.4	12.5	26.41	29.8
183	10.2	79.4	82.5	80.5	14.4	8.1
184	1.8	13.3	9.6	1.5	30.64	3.0
186	37.8	2.0	1.5	5.5	28.41	59.1

days for each of the thermal neutron capture spectra and six to eight days for the average capture spectra. Another spectrum was obtained using a 0.5 g natural abundance sample so that by comparison to that obtained from the 180 mg enriched sample most of the isotopic identifications of the spectral lines were accomplished.

Energy and intensity calibrations of both thermal and average resonance spectra are based primarily on the known lines from the  $^{14}\text{N}(n, \gamma)^{15}\text{N}$  reaction.<sup>26,27</sup> Both before and after the completion of all runs for a given spectral energy range, the through tube which normally contains helium was flushed with nitrogen; and, with the target withdrawn, a nitrogen calibration spectrum was obtained. Also, a 1-day run was taken for each spectrum under the condition that the target is in place while nitrogen is in the through tube. Any significant electronic shifts or count rate effects can be detected with this procedure. The energies were obtained by a method described by

TABLE V. Energy calibration lines for high energy primary transitions.

$E_\gamma$ (keV)	Reaction	Remarks
7299.0 ± 0.5	$^{14}\text{N}(n, \gamma)^{15}\text{N}$	Primary standard <sup>a</sup>
7006.3 ± 0.3	$^{10}\text{B}(n, \gamma)^{11}\text{B}$	Secondary standard <sup>b</sup>
6739.0 ± 0.3	$^{10}\text{B}(n, \gamma)^{11}\text{B}$	Secondary standard <sup>b</sup>
6322.0 ± 0.4	$^{14}\text{N}(n, \gamma)^{15}\text{N}$	Primary standard <sup>a</sup>
5533.2 ± 0.3	$^{14}\text{N}(n, \gamma)^{15}\text{N}$	Secondary standard <sup>a</sup>
5269.2 ± 0.3	$^{14}\text{N}(n, \gamma)^{15}\text{N}$	Primary standard <sup>a</sup>

<sup>a</sup> R. C. Greenwood, Phys. Lett. **27B**, 274 (1968).

<sup>b</sup> G. E. Thomas, Argonne National Laboratory, private communication.

TABLE VI. Primary  $\gamma$ -ray transitions in  $^{184}\text{W}$  following thermal neutron capture in  $^{183}\text{W}$ . Column 2 gives the relative intensity of each  $\gamma$ -ray with the 6408.5 keV line assigned 100.  $E_L = E_0 - E_\gamma$  where  $E_0$ , the ground state transition energy, is  $7411.9 \pm 0.3$  keV.

$E_\gamma$ (keV)	$I_\gamma$	$\frac{\Delta I_\gamma \times 100}{I_\gamma}$	$E_L$ ( $E_0 - E_\gamma$ ) (keV)	$J^\pi$ in level scheme
5007.7 $\pm$ 0.3	10.0	2.0	2404.2 $\pm$ 0.4	0 <sup>+</sup> , 2 <sup>+</sup>
5016.1 $\pm$ 0.3	45.7	1.5	2395.8 $\pm$ 0.4	(1 <sup>+</sup> )
5021.9 $\pm$ 0.3	9.9	2.0	2390.0 $\pm$ 0.4	(1 <sup>+</sup> )
5041.2 $\pm$ 0.3	8.7	2.1	2370.7 $\pm$ 0.4	(1 <sup>+</sup> )
5059.1 $\pm$ 0.3	1.4	8.3	2352.8 $\pm$ 0.4	(1 <sup>-</sup> )
5090.7 $\pm$ 0.3	1.6	6.2	2321.2 $\pm$ 0.4	0 <sup>-</sup> , 2 <sup>-</sup>
5116.9 $\pm$ 0.3	22.0	1.5	2295.0 $\pm$ 0.4	0 <sup>+</sup> , 2 <sup>+</sup>
5164.8 $\pm$ 0.3 <sup>a</sup>	10.0 <sup>a</sup>	3.0	2247.1 $\pm$ 0.5	0 <sup>+</sup> , 2 <sup>+</sup>
5189.2 $\pm$ 0.4	2.7	7.0	2222.7 $\pm$ 0.4	0 <sup>+</sup> , 2 <sup>+</sup>
5243.3 $\pm$ 0.3	14.0	2.4	2168.6 $\pm$ 0.4	1 <sup>+</sup>
5285.0 $\pm$ 0.3	16.0	1.9	2126.9 $\pm$ 0.4	0 <sup>+</sup> , 2 <sup>+</sup>
5307.3 $\pm$ 0.4	2.2	10	2104.6 $\pm$ 0.5	0 <sup>+</sup> , 1 <sup>+</sup> , 2 <sup>+</sup>
5313.8 $\pm$ 0.3	5.0	1.8	2098.1 $\pm$ 0.4	1 <sup>+</sup> , 2 <sup>+</sup>
5321.2 $\pm$ 0.3	6.5 <sup>b</sup>	6.0	2090.7 $\pm$ 0.4	1 <sup>-</sup>
5348.7 $\pm$ 0.3	6.0	5.0	2063.2 $\pm$ 0.4	0 <sup>+</sup> , 2 <sup>+</sup>
5355.1 $\pm$ 0.3	1.0	16	2056.8 $\pm$ 0.4	1 <sup>-</sup>
5375.9 $\pm$ 0.3	4.8	3.6	2036.0 $\pm$ 0.4	2 <sup>+</sup> , 1 <sup>+</sup>
5380.6 $\pm$ 0.3	3.0	9.0	2031.3 $\pm$ 0.4	0 <sup>+</sup> , 2 <sup>+</sup>
5398.6 $\pm$ 0.3	3.0	9.0	2013.3 $\pm$ 0.4	0 <sup>+</sup> , 2 <sup>+</sup>
5415.3 $\pm$ 0.4	0.3	33	1996.6 $\pm$ 0.5	(1 <sup>-</sup> )
5533.6 $\pm$ 1.0 <sup>c</sup>	...	...	1878.3 $\pm$ 1.0	2 <sup>+</sup>
5603.1 $\pm$ 0.3	1.7	4.0	1808.8 $\pm$ 0.4	1 <sup>-</sup>
5636.3 $\pm$ 0.3	4.6	5.0	1775.6 $\pm$ 0.4	(0 <sup>+</sup> ), 2 <sup>+</sup>
5697.7 $\pm$ 0.3	2.4	6.8	1714.2 $\pm$ 0.4	0 <sup>+</sup> , 2 <sup>+</sup>
5783.7 $\pm$ 0.3	5.8	4.0	1628.2 $\pm$ 0.4	1 <sup>+</sup> , (0 <sup>+</sup> , 2 <sup>+</sup> )
5796.9 $\pm$ 0.3	20.6	1.7	1615.0 $\pm$ 0.4	1 <sup>+</sup>
5980.8 $\pm$ 0.3	4.8	2.8	1431.1 $\pm$ 0.4	0 <sup>+</sup> , 2 <sup>+</sup>
6024.2 $\pm$ 0.3	31.9	1.7	1387.7 $\pm$ 0.4	2 <sup>+</sup>
6089.1 $\pm$ 0.3	1.7	6.0	1322.8 $\pm$ 0.4	0 <sup>+</sup> , 2 <sup>+</sup>
6190.6 $\pm$ 0.3 <sup>d</sup>	58.0 <sup>d</sup>	2.2	(1221.3 $\pm$ 0.4)	
6281.5 $\pm$ 0.4	2.8	7.0	1130.4 $\pm$ 0.5	0 <sup>-</sup> , 2 <sup>-</sup>
6289.6 $\pm$ 0.3	59.4	2.2	1122.3 $\pm$ 0.4	2 <sup>+</sup>
6408.5 $\pm$ 0.3	100.0	1.8	1003.4 $\pm$ 0.4	0 <sup>+</sup>
6507.8 $\pm$ 0.3	24.4	2.6	904.1 $\pm$ 0.4	2 <sup>+</sup>
7300.7 $\pm$ 0.3	41.4	4.8	111.2 $\pm$ 0.2	2 <sup>+</sup>
7411.9 $\pm$ 0.3	116.0	1.3	g.s.	0 <sup>+</sup>

<sup>a</sup> Some fraction due to other isotopes of tungsten.

<sup>b</sup> Covered by a strong line from  $^{14}\text{N}(n, \gamma)^{15}\text{N}$ .

<sup>c</sup> Though primarily due to the ground state transition from  $^{182}\text{W}(n, \gamma)^{183}\text{W}$  we are not able to rule out the possibility of some  $^{184}\text{W}$  contribution.

<sup>d</sup> Some small intensity contribution from  $^{182}\text{W}(n, \gamma)^{183}\text{W}$  is suspected.

Strauss, Lenkszus, and Eickholz<sup>28</sup> based on a sliding pulser which corrects for the nonlinearity of the system. As a check on this method, a standard computer routine making use of the calibration lines listed in Table V was employed.

Line intensities have been corrected for the energy dependence of the detector efficiency and have been adjusted to account for the absorption

in 30.5 cm of polyethylene and 1.74 cm of thorium. The thorium was used to limit the singles count rate to a range of from 2000 to 5000 counts/sec, whereas the polyethylene serves primarily to limit detector damage due to fast neutrons.

The results of the analysis of the thermal neutron capture primary  $\gamma$ -ray data are listed in Table VI. The data in this table were used to determine the multipolarities of the transitions.

In comparison to the primary spectra from thermal neutron capture, the higher energy neutron flux used in the  $(\bar{n}, \gamma)$  process creates small line energy shifts and line shape changes due to a small amount of  $p$ -wave capture being mixed in with the  $s$ -wave capture. For these reasons, the thermal capture energy calibration is more accurate. We have used the latter to establish the capture state energy of 7412.1 keV. The level energies ( $E_L$ ) have been calculated using the ground state transition energy  $E_0$ , rather than the capture state energy since the recoil correction varies from 0.16 to 0.07 keV, causing at most a 0.09 keV relative shift over the range of levels listed. This shift is considerably smaller than the error.

#### PRIMARY TRANSITIONS FROM $^{183}\text{W}(\bar{n}, \gamma)^{184}\text{W}$

A 5 g sample of tungsten oxide placed in a carbon target holder containing a 1.27-cm thick boron absorbing sheath is used as a target for the average resonance neutron capture reaction  $^{183}\text{W}(\bar{n}, \gamma)^{184}\text{W}$ . A description of a typical target holder for this kind of reaction is provided by Bollinger and Thomas in Ref. 25.

The boron efficiently absorbs the thermal and low energy neutron flux, leaving a flux broadly distributed with energy so that the energy of a line centroid is increased. The estimate of this increase in this case is about 300 eV. Though the half-width of this distribution is much wider than in the case of the thermal flux, the resulting line broadening is small enough so that the corresponding spectral resolution is quite adequate. In particular, the thermal spectrum resolution varies from 3.5 to 4.5 keV in the energy range from 5 to 7.4 meV, whereas in the average resonance case, the resolution varies from 4.0 to 5.3 keV for the same energy range. The counting time for the average resonance spectrum was about 4 times that for the thermal case. This increased running time may account for some line broadening.

A comparison of the thermal and average resonance spectra for a common energy range can be made by reference to Figs. 4 and 5. Lines coming from the  $^{183}\text{W}(\bar{n}, \gamma)^{184}\text{W}$  reaction are identified by a  $J^\pi$  assignment.

The ground state of  $^{183}\text{W}$  has spin  $\frac{1}{2}$  and negative

parity ( $J_0 = \frac{1}{2}^-$ ). Neutron capture in this state produces both a  $0^-$  and a  $1^-$  state in  $^{184}\text{W}$ . According to Bollinger and Thomas,<sup>25</sup> the ratio of the  $\gamma$ -ray intensity in a path from  $J_i = J_0 + \frac{1}{2}$  to that in a path from  $J_i = J_0 - \frac{1}{2}$  is 1.47 for  $J_0 < \frac{3}{2}$ . The  $I_\gamma$  in Fig. 6 is based on 1.5 for this ratio. As a result the  $E1$  transitions following  $S$ -wave capture will go to  $0^+$ ,  $1^+$ , or  $2^+$  states as described in Fig. 6. These  $E1$  lines will form two intensity groups having a ratio of 5 to 3 (the  $1^+$  corresponding to 5 and the  $0^+$  and  $2^+$  cases corresponding to 3 as seen in Fig. 6). The next most intense group will be  $M1$  transitions to low spin negative parity state. The data from this experiment do not clearly reveal any  $p$ -wave capture and the intensities of  $E2$  transitions are below the sensitivity of the experiment. As in the case for the thermal neutron capture  $\gamma$ -ray primary transitions, two spectral energy ranges having partial overlap were run. The lower range (4.6 to 6.4 MeV) was obtained as the sum of eight

1-day runs while the upper range (5.8 to 7.4 MeV) contains the sum of seven 1-day runs.

The primary transitions energies and their intensities are listed in Table VII. The energy dependence of the intensities has been partially removed by multiplying by  $(E_0/E_\gamma)^4$ . The fourth power has been chosen since it comes closer to producing zero slope straight line fitting to the data than does either a third power or a fifth power reduction. These results are presented in Fig. 7, where the reduced intensity of the primary transitions is plotted on a log scale. The  $E1$  and  $M1$  intensity groups are each delineated by a pair of straight lines whose separation has been fixed so as to yield the theoretical intensity ratio of 5 to 3. These straight lines represent an eyeball fit to the data. The known spin and parity of the ground state and first excited state, i.e.  $0^+$  and  $2^+$ , respectively, provide a means for identifying the lower intensity  $E1$  group, and the 5 to 3 ratio then

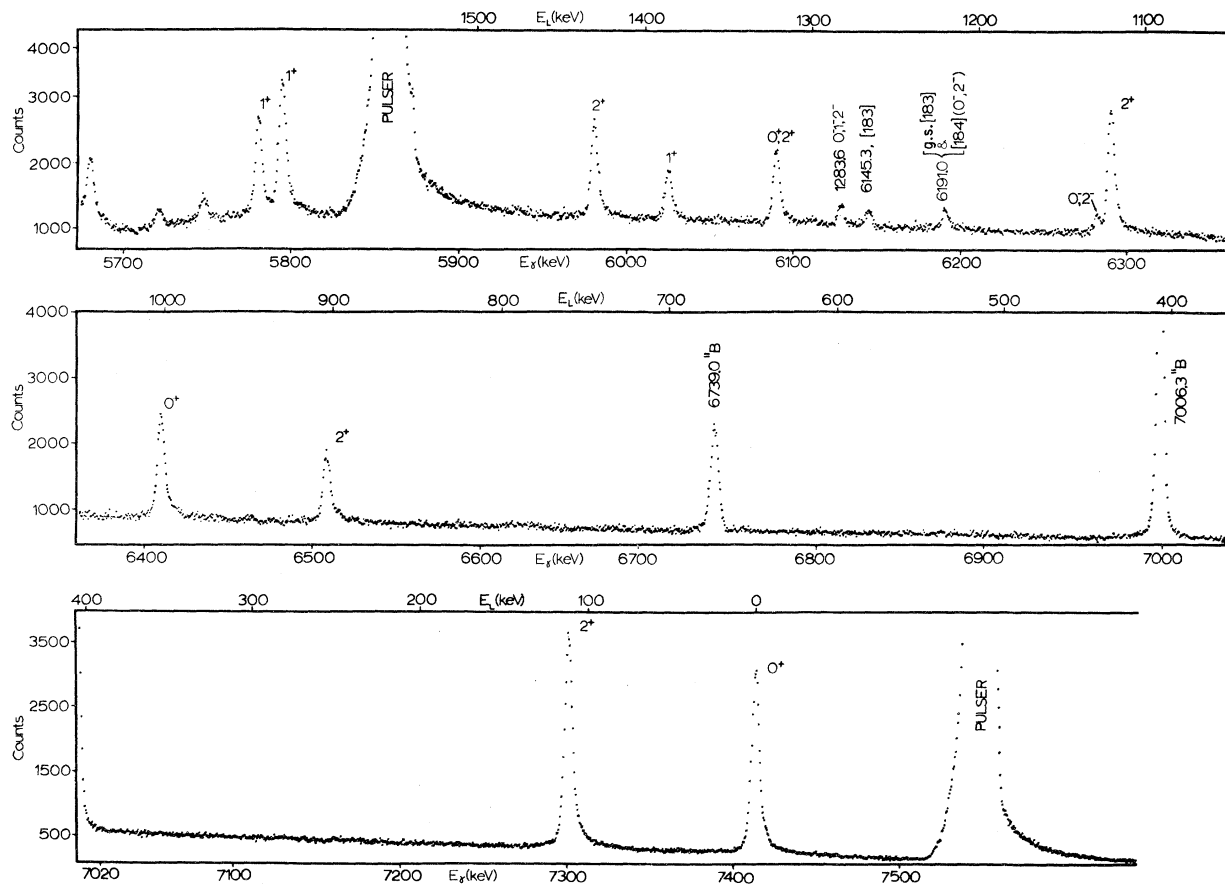


FIG. 4. A spectrum of primary  $\gamma$  transitions following average resonance neutron capture in  $^{183}\text{W}$ . Only double escape peaks appear since the spectrometer electronic system was operated in the coincidence mode. Lines due to transitions in  $^{184}\text{W}$  are marked with a  $J^\pi$  assignment. This spectrum has the higher energy of the two overlapping energy ranges and has an average channel to energy conversion of 0.490 keV/channel.



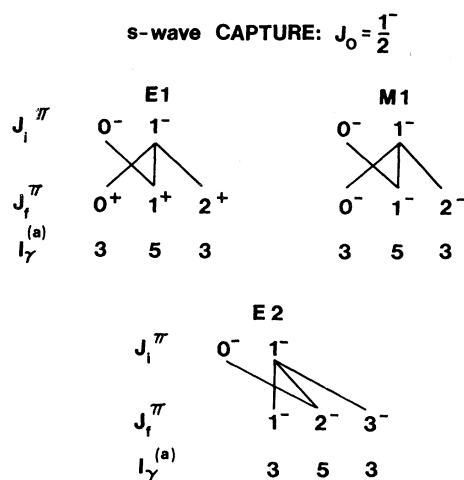


FIG. 6. Decay routes to final states allowed by multipole selection rules for radiations following average resonance neutron capture in  $^{183}\text{W}$ .  $I_\gamma$  is the unnormalized relative intensity.  $J_i$  and  $J_f$  are the initial and final state spin values.  $J_0$  is the ground state spin of  $^{183}\text{W}$ . As explained by L. M. Bollinger and G. E. Thomas (Ref. 25), the ratio of the  $\gamma$ -ray intensity in a path from  $J_i = J_0 + \frac{1}{2}$  to the  $\gamma$ -ray intensity in a path from  $J_i = J_0 - \frac{1}{2}$  is 1.47 for  $J_0 < \frac{3}{2}$ .  $I_\gamma$  is calculated using 1.5 for this ratio.

natural abundance and enriched targets, our evidence for assigning them to transitions in  $^{184}\text{W}$  is weaker than for other lines in the spectrum. However, their appearance only in the  $(\bar{n}, \gamma)$  spectrum from the target enriched in  $^{183}\text{W}$  suggests that  $^{184}\text{W}$  is the only likely candidate of the tungsten isotopes.

The levels suggested by these primary transitions (column 5, Table VII) are used along with low lying levels revealed from  $\gamma$ -ray measurements following  $\beta$  decay to develop the level scheme. The  $J^\pi$  values for these levels based on the results of the intensity analysis of the average resonance primary spectrum, are listed in column 6 of Table VII. As will be seen in the discussion of the level scheme, the spin choices are reduced in some cases by reference to low energy transitions.

#### CAPTURE STATE ENERGIES

The capture state energy for thermal neutron capture is obtained from energy measurements of the primary transitions to the ground state and the first excited state. These transitions were calibrated using the known  $\gamma$ -ray energies from the  $^{14}\text{N}(n, \gamma)^{15}\text{N}$  and  $^{10}\text{B}(n, \gamma)^{11}\text{B}$  reactions. An average from these two transitions after correction for recoil gives a neutron binding energy of  $7412.1 \pm 0.3$  keV.

The estimate of the energy centroid of the capture states formed by average resonance neutron capture is  $7412.3 \pm 0.6$  keV based on the ground state transition corrected for recoil. The error includes a contribution from calibration which was not present in the thermal  $(n, \gamma)$  case.

#### MEDIUM ENERGY SPECTRA

As mentioned briefly before,  $\gamma$ -ray transitions following thermal neutron capture in  $^{183}\text{W}$  form a spectrum in a Ge(Li) detector exhibiting full energy peaks with energies in the range from 500 to 2500 keV (see Fig. 8). Above this range the spectrum is too complicated for meaningful analysis and below 500 keV the line intensities are generally too weak, since the count rate is limited by absorbing the  $\gamma$ -ray beam with thorium having 1.5-cm thickness. Single and double escape peaks are not observed in this spectrum since the antineutrino electronic mode allows only the full energy events to be recorded.<sup>26</sup>

The energies and intensities of these  $\gamma$  rays are listed in Table VIII. Placement of these  $\gamma$  rays in the level scheme is discussed below in the section describing the level scheme.

Isotopic identification of spectral lines in this energy range was also achieved by comparing the natural abundance target spectrum with the enriched target spectrum. The energy calibration lines for these data are listed in Table IX. The full energy peaks of some of the best calibration lines lie above the energy range of this data and so a run in coincidence mode was taken in order to find accurate locations of the double escape peaks of these lines in the lower energy range.

#### LEVEL SCHEMES

The ground state rotational band in  $^{184}\text{W}$  has been described by the  $\beta$ -decay studies of Johnson,<sup>1</sup> Harmatz and Handley,<sup>2</sup> Glatz, Lobner, and Opperman,<sup>3</sup> Kukoc *et al.*,<sup>4</sup> Canty *et al.*,<sup>6</sup> Yates *et al.*,<sup>7</sup> and McMillan *et al.*<sup>8</sup> As stated earlier, our measurements using  $\gamma$ - $\gamma$  coincidence techniques and  $\beta$ -decay excitation are consistent with the conclusions established from these studies. The neutron capture  $\gamma$ -ray excitation process leading to  $^{184}\text{W}$  produces very little direct excitation of states having spins greater than  $J = 2$  because  $J = \frac{1}{2}$  for the ground state spin of  $^{183}\text{W}$  and  $S$ -wave neutron capture predominates. This means that the neutron capture methods provide more limited information for states having spins greater than 2 (i.e., no spin and parity information from average resonance capture). We have made use of the  $(n, \gamma)$

TABLE VII. Primary  $\gamma$ -ray transitions following average-resonance neutron capture in  $^{183}\text{W}$ . The error for  $E_\gamma$  is statistical and does not include the contribution from the calibration process. The ground state transition energy from thermal capture is  $E_0 = 7411.9 \pm 0.3$  keV and from  $(\bar{n}, \gamma)$  the value is  $7412.1 + 0.6$  keV.  $E_L$  in this table is computed using the latter number and  $E_L = E_0 - E_\gamma$ . Parentheses around a level energy or a multipolarity or  $J^\pi$  assignment indicates uncertainty in the existence of the level or in the assignment listed.

$E_\gamma$ (keV)	$I_\gamma (E_0/E_\gamma)^4$	$\frac{\Delta I \times 100}{I}$	Multipole	$E_L$ ( $E_0 - E_\gamma$ ) (keV)	$J^\pi$ via $(\bar{n}, \gamma)$
5008.2 ± 0.4	48	19	E1	2404.8	0 <sup>+</sup> , 2 <sup>+</sup>
5016.6 ± 0.3	71	13	E1	2395.5	(1 <sup>+</sup> )
5022.8 ± 0.3	70	14	E1	2389.3	(1 <sup>+</sup> )
5042.1 ± 0.3	65 <sup>a</sup>	14	E1	2370.0	(1 <sup>+</sup> )
5059.5 ± 0.4	16	38	M1	2352.6	(1 <sup>-</sup> )
5090.7 ± 0.9	7	60	(M1)	(2321.4)	0 <sup>-</sup> , 2 <sup>-</sup>
5117.4 ± 0.3	42	16	E1	2294.7	0 <sup>+</sup> , 2 <sup>+</sup>
5165.5 ± 0.3	49 <sup>b</sup>	20	E1	2246.6	0 <sup>+</sup> , 2 <sup>+</sup>
5189.9 ± 0.3	46	14	E1	2222.2	0 <sup>+</sup> , 2 <sup>+</sup>
5244.1 ± 0.1	94	8	E1	2168.0	1 <sup>+</sup>
5285.6 ± 0.4	41	14	E1	2126.5	0 <sup>±</sup> , 2 <sup>+</sup>
5300.9 ± 0.5	34	16	E1	2111.2	0 <sup>+</sup> , 2 <sup>+</sup>
5307.9 ± 0.2	63	10	E1	2104.2	0 <sup>+</sup> , 2 <sup>+</sup> , 3 <sup>+</sup>
5314.3 ± 0.2	77	9	E1	2097.8	1 <sup>+</sup>
5322.1 ± 0.4	19 <sup>c</sup>	27	M1	2090.0	1 <sup>-</sup>
5327.3 ± 0.5 <sup>d</sup>	7.5	64	M1	2084.8	0 <sup>-</sup> , 2 <sup>-</sup>
5338.1 ± 0.6 <sup>d</sup>	5.2	95	M1	(2074.0)	(0 <sup>-</sup> , 2 <sup>-</sup> )
5348.7 ± 0.3	45	13	E1	2063.4	0 <sup>+</sup> , 2 <sup>+</sup>
5356.7 ± 0.6	12	45	M1	2055.4	0 <sup>-</sup> , 1 <sup>-</sup> , 2 <sup>-</sup>
5376.4 ± 0.3	57	11	E1	2035.7	0 <sup>+</sup> , 2 <sup>+</sup> , 1 <sup>+</sup>
5381.1 ± 0.3	43 <sup>e</sup>	13	E1	2031.0	0 <sup>+</sup> , 2 <sup>+</sup>
5398.8 ± 0.3	50	12	E1	2013.3	0 <sup>+</sup> , 2 <sup>+</sup>
5417.8 ± 0.6	6.1 <sup>a</sup>	80	(M1)	(1994.3)	(0 <sup>-</sup> , 2 <sup>-</sup> )
5534.9 ± 0.5	42	15	E1	1877.2	0 <sup>+</sup> , 1 <sup>+</sup> , 2 <sup>+</sup>
5603.5 ± 0.4	23	18	(M1)	1808.6	(1 <sup>-</sup> )
5636.7 ± 0.2	54	10	E1	1775.4	(0 <sup>+</sup> ), 2 <sup>+</sup>
5697.5 ± 0.4	48	10	E1	1714.6	0 <sup>+</sup> , 2 <sup>+</sup>
5783.9 ± 0.1	84	5	E1	1628.2	1 <sup>+</sup>
5796.7 ± 0.2	84	4	E1	1615.4	1 <sup>+</sup>
5798.3 ± 0.7	45	20	E1	1613.8	0 <sup>+</sup> , 2 <sup>+</sup>
5980.9 ± 0.1	68 <sup>b</sup>	5	E1	1431.2	0 <sup>+</sup> , 2 <sup>+</sup>
6025.2 ± 0.2	30	9	M1 or E1	1386.9	1 <sup>-</sup> , 2 <sup>+</sup>
6089.7 ± 0.2	45	5	E1	1322.4	0 <sup>+</sup> , 2 <sup>+</sup>
6128.5 ± 0.3 <sup>d</sup>	12	16	M1	1283.6	0 <sup>-</sup> , 1 <sup>-</sup> , 2 <sup>-</sup>
6191.0 ± 0.4	12 <sup>f</sup>	16	(E2)	1221.1	(1 <sup>-</sup> , 2 <sup>-</sup> , 3 <sup>-</sup> )
6282.0 ± 0.5	9.2	17	M1	1130.1	0 <sup>-</sup> , 2 <sup>-</sup>
6290.2 ± 0.1	79	4	E1	1121.9	2 <sup>+</sup>
6409.4 ± 0.1	65	4	E1	1002.7	0 <sup>+</sup>
6508.5 ± 0.3	41	5	E1	903.6	2 <sup>+</sup>
7300.2 ± 0.1	100	3	E1	111.9	2 <sup>+</sup>
7412.1 ± 0.1	78	3	E1	0.0	0 <sup>+</sup>

<sup>a</sup> This transition has a contribution from another isotope.

<sup>b</sup> This transition has a contribution from another isotope which has been removed.

<sup>c</sup> This transition has a contribution from  $^{186}\text{W}(\bar{n}, \gamma)^{187}\text{W}$ .

<sup>d</sup> Isotopic identification is not definite but  $^{183}\text{W}(\bar{n}, \gamma)^{184}\text{W}$  is most likely.

<sup>e</sup> May have a small contribution from  $^{184}\text{W}(\bar{n}, \gamma)^{185}\text{W}$ .

<sup>f</sup> We estimate 7.8 due to ground state transition in  $^{183}\text{W}$  and 4.5 due to  $^{184}\text{W}$ .

process to describe the low spin ( $J \leq 2$ ) states of the level scheme to an energy of about 2.5 MeV, almost 1 MeV above the last state excited by the  $\beta$ -decay process.

The partial level scheme shown in Fig. 9 is based on the capture  $\gamma$ -ray measurements and features 38 levels above 1 MeV, four of which are uncertain and indicated with a dashed line. The result-

ing average level spacing is 39 keV in this energy region. This is a sufficiently large spacing so that accidental fits of the transitions between levels should not be a serious problem. Even so there are 5 out of 52  $\gamma$ -ray placements that can be placed in more than one location. Only 10 of the 58  $\gamma$  rays listed in Table VIII having energies less than 2404 keV have not been placed in the level scheme.

In general, the development of the  $^{184}\text{W}$  level scheme is guided by the results of levels predicted by primary transitions following average resonance neutron capture as seen in Table VII. The thermal neutron capture data is used to corroborate the results of the average resonance data and aid in identification of impurities.

Due to the nature of the  $(\bar{n}, \gamma)$  processes the  $E1$  primary transitions to low spin (0, 1, and 2) positive parity states are very intense and about five times more intense than the  $M1$  transitions (see Fig. 7) when reduced intensities are compared (column 2, Table VII). This means that even if an intensity falls in between these two groups (the  $E1$  and  $M1$  groups of Fig. 7) due to some residual Porter-Thomas fluctuation, it will be detected unless it is overlooked in a close doublet or multiplet structure or identified incorrectly as to isotopic origin. Thus, unless lost in a multiplet or incorrectly identified, all the positive parity states

are observed. In addition, only very few of them (two in the case of  $^{184}\text{W}$ ) fall between the two groups, leading to some uncertainty in choice of parity. A summary of the levels in the two level schemes (Figs. 3 and 9) is provided in Table X.

#### Ground state rotational band

This band has been well described by many previous investigations referred to in this paper and our description of these levels are consistent with these earlier studies. For instance, we observe strong average resonance neutron capture primary transitions to the  $0^+$  ground state and the  $2^+$  first excited state while such transitions to the first  $4^+$  state and  $6^+$  state are not observed. As discussed before, it is the nature of the  $(n, \gamma)$  process for this case for primary transitions to reach states whose spins are  $\leq 2$  only.

Level at  $903.2 \pm 0.2$  keV:  $J^\pi = 2^+$

There is ample evidence from previously reported work<sup>1-8</sup> for a level at this energy so that it can be considered a well-established level. Our  $\beta$ -decay data shows 750 times more  $\gamma$ -ray intensity out than into this level, which is possible because of  $\beta$  decay directly to this state.

As seen in Fig. 7, the  $E1$  group into which the

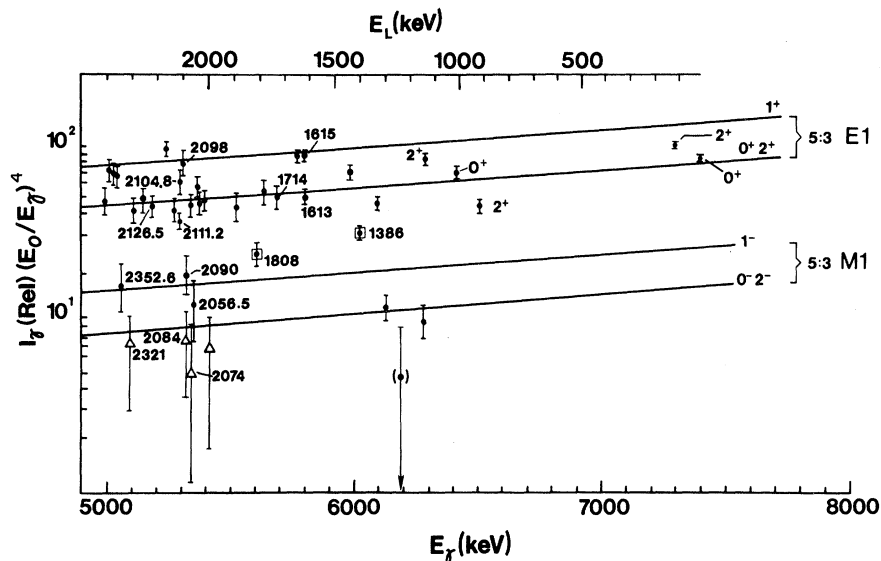


FIG. 7. A plot of the reduced primary  $\gamma$  transition intensity with energy for average resonance neutron capture in  $^{183}\text{W}$ . Each set of two lines has been spaced to reflect the predicted 5 to 3 intensity ratio (see Fig. 6) and then moved to obtain a fit to the data. The points plotted with open triangles correspond to the states dashed in the level scheme. Except for the extreme cases, the spin groups do not separate distinctly. Thus spin 1 can only be distinguished in a few cases from spins of 0 and 2. Except for two cases plotted with squares the positive parity cases separate distinctly from the negative parity cases. A number shown beside a plotted point is the level energy for a state having a special discussion in the text. A possible  $E2$  transition at 6191 keV is shown in parentheses.

average resonance primary transition falls in the  $0^+$ ,  $2^+$  group; however, the averaging appears to be unusually weak in this case. In light of the three transitions shown in the decay scheme (Fig. 3) and the two transitions placed in the level scheme based on  $(n, \gamma)$  data only (Fig. 9), an assignment of 0 for spin is ruled out; therefore  $J^\pi = 2^+$ .

The energy of  $903.2 \pm 0.2$  keV is obtained from the transitions to final states shown in Fig. 9, which is consistent with the values obtained from primary  $(\bar{n}, \gamma)$  and  $(n, \gamma)$  data (see Tables VI and VII) as well as the  $\beta$ -decay results (Fig. 3).

Level at  $1002.8 \pm 0.3$  keV:  $J^\pi = 0^+$

Our  $\beta$ -decay experiments provide no evidence for this level; however, primary  $(n, \gamma)$  transitions

listed in Tables VI and VII indicate an  $E1$  transition, and reference to Fig. 7 shows that the spin and parity possibilities are  $0^+$  and  $2^+$ . The strong 891.5 keV  $\gamma$  ray to the  $2^+$  excited state, along with the absence of transitions to the  $0^+$  ground state and  $4^+$  second excited state, suggests that the proper choice is  $J^\pi = 0^+$ .

Measurements reported independently in 1968 by Faler, Spencer, and Harian<sup>13</sup> and by Alves *et al.*<sup>10</sup> suggested a  $0^+$  state at about this energy, to be distinguished from a nearby  $3^+$  state found by previous  $\beta$ -decay studies (see below). A much earlier  $(n, \gamma)$  experiment conducted by Bollinger *et al.*<sup>29</sup> revealed a state at 1001 keV which was probably this state. In the work by Faler *et al.*<sup>13</sup> capture in the 7.6 eV resonance of  $^{183}\text{W}$  leading to

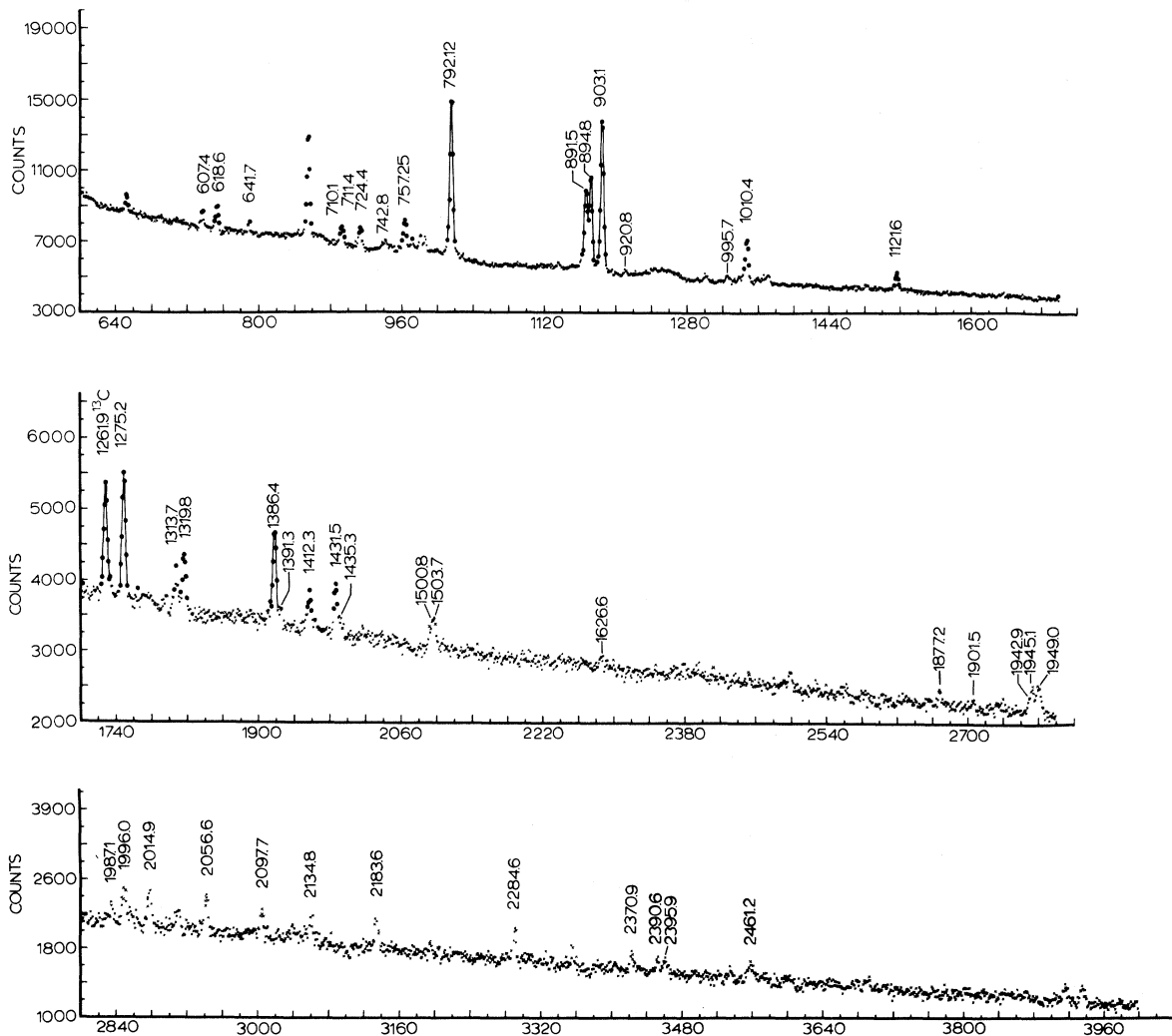


FIG. 8. (a) Medium energy  $\gamma$ -ray spectrum following thermal capture in  $^{183}\text{W}$ . This spectrum is made of full energy peaks by use of the spectrometer anticoincidence mode. (b) Medium energy  $\gamma$ -ray spectrum following thermal capture in natural abundance tungsten.

TABLE VIII. Medium energy  $\gamma$  rays from cascades in  $^{184}\text{W}$  following thermal neutron capture in  $^{183}\text{W}$ . Measurements are obtained using a Ge(Li) spectrometer with Compton and escape peak suppression.  $I_\gamma$  is the relative intensity normalized to 100 for the 792.12 keV line. A transition whose placement is uncertain is indicated by a yes in parenthesis in column 3. The number in parentheses after "yes" in column 3 indicates the number of alternative placements in the level scheme.

$E_\gamma$ (keV)	$I_\gamma$	Placed in scheme	Remarks
607.4 $\pm$ 0.2	10 $\pm$ 2	yes (2)	
618.6 $\pm$ 0.6	1.0 $\pm$ 0.6	(yes)	
641.7 $\pm$ 0.1	4.4 $\pm$ 0.8	yes	
710.1 $\pm$ 0.3	7 $\pm$ 1	yes (2)	
711.4 $\pm$ 0.3	4 $\pm$ 1	yes	
724.4 $\pm$ 0.1	12 $\pm$ 1	yes	
742.8 $\pm$ 0.3	4.1 $\pm$ 0.8	yes	
757.25 $\pm$ 0.06	19 $\pm$ 1	yes	
766.0 $\pm$ 0.6	2 $\pm$ 1	yes	} Quadruplet structure
769.33 $\pm$ 0.1	12 $\pm$ 1	yes (2)	
771.4 $\pm$ 0.6	2 $\pm$ 1	yes	
792.12 $\pm$ 0.06	100 $\pm$ 2	yes	
796.5 $\pm$ 0.2	3 $\pm$ 1	no	
880.9 $\pm$ 0.6	3 $\pm$ 1	no	
891.5 $\pm$ 0.2	47 $\pm$ 1	yes	Possible close doublet
894.8 $\pm$ 0.1	54 $\pm$ 1	yes	
903.1 $\pm$ 0.1	97 $\pm$ 2	yes	
920.8 $\pm$ 0.2	4 $\pm$ 1	no	
980.5 $\pm$ 0.3	3.4 $\pm$ 0.5	(yes)	Uncertain identification
995.7 $\pm$ 0.3	4 $\pm$ 1	yes	Uncertain identification
1005.3 $\pm$ 0.4	3 $\pm$ 1	(yes)	Uncertain identification
1010.4 $\pm$ 0.1	28 $\pm$ 1	yes	
1022.5 $\pm$ 0.8 <sup>a</sup>	3.5 $\pm$ 0.5	yes (2)	Resolved from doublet
1099.5 $\pm$ 0.8	2 $\pm$ 1	yes	
1109.8 $\pm$ 1.2	1 $\pm$ 0.5	(yes)	Uncertain identification
1121.6 $\pm$ 0.3	10 $\pm$ 1	yes	
1265.5 $\pm$ 0.6	1 $\pm$ 0.5	(yes)	Uncertain identification
1275.2 $\pm$ 0.1	20 $\pm$ 1	yes	
1313.7 $\pm$ 0.4	5 $\pm$ 1	no	
1319.8 $\pm$ 0.2	8.6 $\pm$ 0.8	yes (2)	
1386.4 $\pm$ 0.1	14 $\pm$ 1	yes	
1391.3 $\pm$ 0.7	3 $\pm$ 1	yes	
1412.3 $\pm$ 0.5 <sup>a</sup>	5.8 $\pm$ 0.8	yes	Unfolded from triplet structure
1431.5 $\pm$ 0.3	7.9 $\pm$ 0.9	yes	
1435.3 $\pm$ 0.5	1.8 $\pm$ 0.9	no	
1500.8 $\pm$ 0.3	3.2 $\pm$ 0.1	yes (2)	Uncertain identification
1503.7 $\pm$ 0.2	4.6 $\pm$ 0.9	yes	
1626.6 $\pm$ 0.3	1.5 $\pm$ 0.8	(yes)	
1766.5 $\pm$ 0.3 <sup>a</sup>	2.9 $\pm$ 0.5	yes	
1877.2 $\pm$ 0.3	2.3 $\pm$ 0.5	yes	
1901.9 $\pm$ 0.3	1.3 $\pm$ 0.4	yes	$^{184}\text{W}$ plus another source
1942.9 $\pm$ 0.5	9.8 $\pm$ 0.6	no	
1945.1 $\pm$ 0.3	3.8 $\pm$ 0.8	yes	
1949.0 $\pm$ 0.4	2.2 $\pm$ 0.7	no	
1951.2 $\pm$ 0.3	3.4 $\pm$ 0.8	yes	
1987.1 $\pm$ 0.4	1.9 $\pm$ 0.8	yes	
1996.0 $\pm$ 0.3	4.3 $\pm$ 0.7	yes	
2000.6 $\pm$ 0.6	1.0 $\pm$ 0.6	no	
2004.8 $\pm$ 0.7	0.6 $\pm$ 0.8	no	
2014.9 $\pm$ 0.3	4.6 $\pm$ 0.7	(yes)	
2036.0 $\pm$ 0.3	2.3 $\pm$ 0.7	yes	
2056.6 $\pm$ 0.3	4.6 $\pm$ 0.7	yes (2)	
2097.7 $\pm$ 0.3	3.4 $\pm$ 0.7	yes	
2134.8 $\pm$ 0.6	2.5 $\pm$ 0.8	yes	

TABLE VIII (Continued)

$E_\gamma$ (keV)	$I_\gamma$	Placed in scheme	Remarks
2183.6 $\pm$ 0.3	3.9 $\pm$ 0.8	yes	
2284.6 $\pm$ 0.2	4.3 $\pm$ 0.6	yes	
2370.9 $\pm$ 0.4	2.3 $\pm$ 0.7	(yes)	Uncertain identification
2390.6 $\pm$ 0.5	1.6 $\pm$ 0.6	(yes)	Uncertain identification
2395.9 $\pm$ 0.5	1.6 $\pm$ 0.6	(yes)	Uncertain identification
2461.2 $\pm$ 0.5	0.8 $\pm$ 0.7	no	Uncertain identification
2690.0 $\pm$ 0.5	1.8 $\pm$ 0.6	no	Uncertain identification

<sup>a</sup> Some fraction of these lines may be due to other isotopes. The intensity ratios between the enriched and natural abundance target cases for these lines are close enough to the expected ratio so that it is definite that there is a  $^{184}\text{W}$  contribution but another smaller contribution to the listed intensity from another source cannot be ruled out.

primary transitions from the capture state are used with coincidence methods to gate low energy spectra resulting from the same reaction. Their results indicate that an 893 keV transition is in coincidence with the 6409 keV primary transition. Our medium energy  $\gamma$ -ray spectrum has both an 891.5 and 894.8 keV transition. Their 893 keV  $\gamma$  ray very likely corresponds to the former. Comparison of their four listed  $\gamma$ -ray energies with ours indicates about a 1.5 keV systematic shift between the two calibrations. More recently,  $(n, \gamma)$  studies<sup>11, 15, 16</sup> and  $(d, p)$  work<sup>20</sup> have supported the existence of the  $0^+$  state.

Level at 1005.9  $\pm$  0.2 keV:  $J^\pi = 3^+, 4^+$

Our  $\beta$ -decay coincidence spectra provide evidence for a level at 1005.9  $\pm$  0.2 keV having transitions to the  $2^+$  state at 111.24 keV and the  $4^+$  state at 364.1 keV. Primary transitions following average resonance neutron capture or thermal neutron capture are not observed to this state, suggesting a spin greater than 2. The 641.9 keV  $\gamma$  ray is observed in spectra gated by both the 111.24 keV  $\gamma$  ray and the 252.8 keV  $\gamma$  ray while the much stronger 894.8 keV  $\gamma$  ray is observed only in the case of the 111.24 keV gated spectrum. We conclude that the  $J^\pi$  assignment should be either  $3^+$  or  $4^+$ . Kukoc *et al.*<sup>4</sup> made a case for a  $3^+$  state at this energy, and this has subsequently been verified by additional  $\beta$ -decay studies<sup>6-8</sup> and by  $(d, p)$  reactions.<sup>20</sup>

Level at 1121.5  $\pm$  0.4 keV:  $J^\pi = 2^+$

The intensity ratios among  $\gamma$ -ray transitions depopulating this state are virtually identical whether obtained from  $\beta$ -decay data or from neutron capture data. This is also true of the two-level energy values obtained from the two sets of data.

The  $E1$  primary transition to this state, coupled with the set of three transitions drawn in Fig. 9, suggests a  $2^+$  spin and parity assignment. This is supported by the work of Faler *et al.*<sup>13</sup> which employs coincidence gating of primary transitions. The ratios of intensities between the 1121.6 keV (10%), 1010.4 keV (28%), and 757.2 keV (19%) transitions observed in the  $(n, \gamma)$  data are 1:2.8:1.9, and from our  $\beta$  decay they are 1:2.6:1.9. These ratios agree within error uncertainties with those reported by Faler *et al.*<sup>13</sup> (1:2.0:1.9) from  $(n, \gamma)$  and by Kukoc *et al.*<sup>4</sup>

TABLE IX. Calibration lines for the medium energy spectrum. Except for the first line listed, all calibration lines come from the  $^{14}\text{N}(n, \gamma)^{15}\text{N}$  reaction. The double escape peaks of the  $^{15}\text{N}$  lines are used to calibrate the full energy peaks of the  $^{184}\text{W}$  lines so the corresponding detector energies are listed in column 2. The two primary standards were used with the ramp generator technique to obtain the calibration of the spectrum by use of a computer. The secondary standard provided a check on the success of the calibration and means for preliminary hand calculations.

$E_\gamma$ <sup>a</sup> (keV)	Detector energy (keV) $E_\gamma - 2mc^2$	Remarks
1261.92 $\pm$ 0.06 <sup>b</sup>		Secondary standard
1884.41 $\pm$ 0.10	862.81 $\pm$ 0.06	Primary standard
1999.65 $\pm$ 0.10	977.65 $\pm$ 0.10	Secondary standard
2520.55 $\pm$ 0.10	1498.55 $\pm$ 0.10	Secondary standard
2831.1 $\pm$ 0.2	1809.1 $\pm$ 0.2	Secondary standard
3532.2 $\pm$ 0.2	2510.2 $\pm$ 0.2	Primary standard
3677.7 $\pm$ 0.2	2655.7 $\pm$ 0.2	Secondary standard

<sup>a</sup> The energy values for the  $\gamma$  rays from the  $^{14}\text{N}(n, \gamma)^{15}\text{N}$  reaction were obtained from R. C. Greenwood, Phys. Lett. **27B**, 274 (1968).

<sup>b</sup> This line comes from the  $^{12}\text{C}(n, \gamma)^{13}\text{C}$  reaction and the value comes from W. V. Prestwich, R. E. Coté, and G. E. Thomas, Phys. Rev. **161**, 1080 (1967).

(1:3.9:3) from  $\beta$ -decay work. The ratios from the recent  $(n, \gamma)$  study by Greenwood and Reich<sup>11</sup> are (1:3.6:2.7) and from the  $\beta$  decay by McMillan *et al.*<sup>8</sup> they are (1:2.6:1.8).

Level at  $1130.1 \pm 0.7$  keV:  $J^\pi = 2^-$

The evidence for this level is based on an  $M1$  average resonance neutron capture primary  $\gamma$  transition which suggests a value of  $J^\pi = 0^-$  or  $2^-$  (see Table VII) and on a weak primary transition following thermal capture (see Table VI). We have not observed secondary transitions from thermal capture that can be connected to this level. However, transitions following  $\beta$  decay of energies 1017.5 and 226.1 keV have been assigned to a level at  $1129.4 \pm 0.6$  keV as seen in Fig. 3. The 1017.5 keV is dashed in that level scheme since it was observed only in a coincidence spectrum. These transitions suggest that a  $2^-$  assignment is more likely than a  $0^-$ . This is consistent with the con-

clusions based on  $\beta$ -decay measurements<sup>6-8</sup> as well as on  $(n, \gamma)$  experiments.<sup>11</sup>

Level at  $1133.6 \pm 0.3$  keV:  $J^\pi = 4^+$

The energy and assignment is based on the two transitions to the first  $2^+$  and the first  $4^+$  states and on the failure to observe primary transitions following average neutron capture. The  $4^+$  assignment agrees with the results from many previous authors (Refs. 6-8, 11, 16, 17, 20, 21).

Level at  $1221.5 \pm 0.4$  keV:  $J^\pi = (3^-)$

Our  $\beta$ -decay results indicate three  $\gamma$  transitions from this state (see Fig. 3), all having the longer half-life of the 169-day metastable state in <sup>184</sup>Re. The two transitions to  $2^+$  states limit the spin to 3 or below, and the transition to the 1005.9 keV state suggests that the spin is more than 1.

Our average capture data reveals a possible  $E2$  transition of 6191.0 keV (see Table VII). Since it

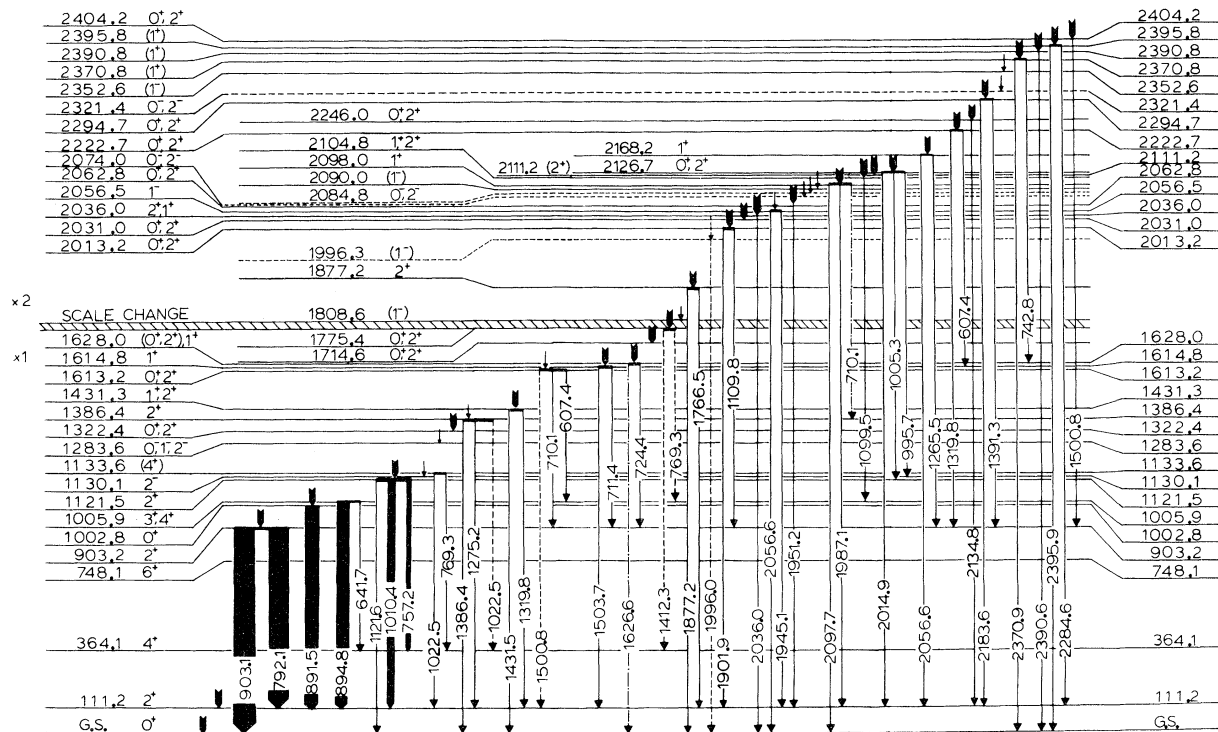


FIG. 9. The level scheme for <sup>184</sup>W based on neutron-capture  $\gamma$ -ray spectroscopy. A  $\gamma$  transition given as a dot-dash line has been placed with a rather poor energy fit. A dashed transition comes from a dashed level, that is from a level whose existence is uncertain. The heavy short arrows located on initial states represent the  $E1$  average resonance primary transitions from the capture state. The short thin arrows signify the  $M1$  primary transitions. Parentheses around a  $J^\pi$  assignment indicates that the  $J$  value is tentative [for instance at 2111.2 keV the  $(2^+)$  located to the right of the energy value means a tentative spin assignment of 2 and a definite positive parity assignment]. However, at 1628.0 keV the parentheses means that spins of 0 and 2 are not ruled out but are of lesser likelihood than  $J=1$ . The  $J^\pi$  assignments are based on our  $(n, \gamma)$  data only, except for the  $4^+$  and  $6^+$  states in the ground state band. This means that there are a few cases in which more definitive assignments are available in the literature. These are discussed in the text.

TABLE X. Levels in  $^{184}\text{W}$  deduced from neutron capture data and  $\beta$ -decay data. The errors shown for neutron capture are statistical and do not reflect calibration uncertainties.

Neutron capture		$\beta$ decay	
$E_L$ (keV)	$J^\pi$	$E_L$ (keV)	$J^\pi$
g.s.	$0^+$		
$111.2 \pm 0.2$	$2^+$	$111.24 \pm 0.06$	$2^+$
		$364.08 \pm 0.07$	$4^+$
		$748.1 \pm 0.4$	$6^+$
$903.3 \pm 0.2$	$2^+$	$903.3 \pm 0.2$	$2^+$
$1002.8 \pm 0.3$	$0^+$		
		$1005.9 \pm 0.2$	$(3^+)$
$1121.5 \pm 0.4$	$2^+$	$1121.5 \pm 0.5$	$2^+$
$1130.1 \pm 0.4$	$2^-$	$1129.4 \pm 0.6$	$2^-$
$1133.6 \pm 0.5$	$(4^+)$	$1133.8 \pm 0.6$	$4^+$
$[1221.1 \pm 0.4$	$1^-, 2^-, 3^-]^a$	$1221.7 \pm 0.4$	$(2^-, 3^-)$
$1283.6 \pm 0.7$	$0^-, 1^-, 2^-$		
		$1285.1 \pm 0.6$	$(5^-)$
$1322.4 \pm 0.4$	$0^+, 2^+$		
$1386.4 \pm 0.2$	$2^+$	$1386.5 \pm 0.3$	$1^+, 2^+$
$1431.3 \pm 0.3$	$1^+, 2^+$	$1430.5 \pm 0.5$	$1^+, 2^+$
		$1501.1 \pm 0.4$	$(7^-)^b$
$1613.2 \pm 0.5$	$0^+, 2^+$		
$1614.8 \pm 0.2$	$1^+$		
$1628.0 \pm 0.4$	$1^+, (0^+, 2^+)$		
$1714.6 \pm 0.4$	$0^+, 2^+$		
$1775.4 \pm 0.6$	$0^+, 2^+$		
$1808.6 \pm 0.4$	$1^-$		
$1877.2 \pm 0.5$	$2^+$		
$1996.3 \pm 0.5$	$(1^-)$		
$2013.2 \pm 0.2$	$0^+, 2^+$		
$2031.0 \pm 0.4$	$0^+, 2^+$		
$2036.0 \pm 0.3$	$1^+, 2^+$		
$2056.5 \pm 0.3$	$1^-$		
$2062.8 \pm 0.3$	$0^+, 2^+$		
$2074.0 \pm 0.7$	$0^-, 2^-$		
$2084.8 \pm 0.8$	$0^-, 2^-$		
$2090.0 \pm 0.8$	$1^-$		
$2098.0 \pm 0.3$	$1^+$		
$2104.8 \pm 0.6$	$0^+, 1^+, 2^+$		
$2111.2 \pm 0.6$	$0^+, 2^+$		
$2126.7 \pm 0.4$	$0^+, 2^+$		
$2168.2 \pm 0.4$	$1^+$		
$2222.7 \pm 0.4$	$0^+, 2^+$		
$2246.0 \pm 0.4$	$0^+, 2^+$		
$2294.7 \pm 0.4$	$0^+, 2^+$		
$2321.4 \pm 0.9$	$0^-, 2^-$		
$2352.6 \pm 0.4$	$(1^-)$		
$2370.8 \pm 0.4$	$(1^+)$		
$2390.8 \pm 0.3$	$(1^+)$		
$2395.8 \pm 0.4$	$(1^+)$		
$2404.2 \pm 0.4$	$0^+, 2^+$		

<sup>a</sup> Has not been included in the level scheme based on  $(n, \gamma)$  data since the primary transitions to this state are not definitely identified.

<sup>b</sup> Adapted from Refs. 3 to 8.

is composite with the ground state transition from  $^{182}\text{W}(\bar{n}, \gamma)^{183}\text{W}$  so that only 4.5 ( $\pm 100\%$ ) of its 12.3 units of reduced relative intensity are assigned to  $^{184}\text{W}$ , its existence is in doubt. Positive parity is ruled out. This intensity is weak enough to be a possible  $E2$  and essentially too weak to be an  $M1$  transition. Since the spin must be greater than 1, we conclude possible  $J^\pi$  values of  $2^-$  or  $3^-$  (see Fig. 6). Though we can not distinguish between spin 2 and spin 3, other authors<sup>7,17</sup> have concluded that  $J^\pi = 3^-$  for this level. Due to the limitations of the  $(\bar{n}, \gamma)$  evidence for this level we have not included it in Fig. 9. We have a once-placed 1109.8 keV  $\gamma$  ray (see Table VIII) which might properly be placed at this level as suggested by Greenwood and Reich.<sup>11</sup> We have no evidence for the nearby positive parity state at 1226 keV reported by Samour *et al.*<sup>15</sup> with suggested spin choices of 0, 1, or 2.

Levels at  $1283.6 \pm 0.7$  keV:  $J^\pi = 0^-$ ,  
 $1^-$ ,  $2^-$ , and at  $1285.1 \pm 0.6$  keV:  $J^\pi = 5^-$

Study of  $\beta$ -decay excitation of a level at 1285.1 keV suggests that it is fed directly from the  $8^+$  metastable state of  $^{184}\text{Re}$ . Two transitions (1173.8 and 921.1 keV) of the three which we have assigned to a state at 1285 keV (see Fig. 3) are verified by our coincidence data and all three have the longer half-life corresponding to the  $8^+$  state in  $^{184}\text{Re}$  (see Table II). As previously pointed out, a number of authors<sup>2-4,6-8,11,17</sup> have concluded that the spin and parity assignment to this level should be  $5^-$ . Since a spin of 5 is likely to be too high to be observed in the primary neutron capture  $\gamma$ -ray spectra, there must be two levels involved—one which is excited by the  $\beta$  decay and the other by neutron capture at 1283.6 keV.

The 920.8 keV  $\gamma$  ray in the  $(n, \gamma)$  spectrum (see Table VIII) is probably coming from the  $5^-$  state at 1285.1 keV, since it is not compatible with the range of spin-parity values ( $0^-, 1^-, 2^-$ ) suggested by the  $M1$  primary capture  $\gamma$  ray to the 1283.6 keV state (see Fig. 9). Our measurements from the  $\beta$ -decay work show that the 1173.8 keV line is nine times weaker than the 921 keV line placing it below the limit of sensitivity of the medium energy  $(n, \gamma)$  spectrum, consistent with the fact that it is not observed in the  $(n, \gamma)$  spectrum.

A recent study done by Krane *et al.*<sup>24</sup> suggests that there is admixing by way of a weak interaction with a nearby level of opposite parity; therefore, the level detected by average resonance neutron capture  $\gamma$ -ray spectroscopy is not that level.

Level at  $1322.4 \pm 0.4$  keV:  $J^\pi = 0^+, 2^+$

The strength of the primary transition following average resonance neutron capture (see Fig. 7)

strongly suggests that a level having  $J^\pi = 0^+$  or  $2^+$  is located at an energy of 1322.4 keV. A level at this energy is reported by Günther *et al.*<sup>17</sup> based on inelastic scattering of 12 MeV deuterons; however, they did not make a  $J^\pi$  assignment. Also, Greenwood and Reich<sup>11</sup> suggested a  $0^+$  at this energy.

Level at  $1386.4 \pm 0.2$  keV:  $J^\pi = 2^+$

The average resonance transition to this state has a multipolarity of either  $E1$  or  $M1$ , since its intensity falls between the  $M1$  and  $E1$  groups (see Fig. 7). If the transition is an  $M1$  we should make an assignment of  $1^-$  and, if an  $E1$ , then a  $2^+$  assignment is expected. Both assignments are compatible with the transitions to the ground state and first excited state shown in the level scheme (Fig. 9). One other transition is observed from this level based on the  $\beta$ -decay data (see Table II and Fig. 3); however, its energy of 482.4 keV is below the range of the medium energy capture  $\gamma$ -ray data. The two intensity ratios (one from the  $\beta$ -decay measurement and the other from the capture data) of the 1386.4 and 1275.2 keV transitions are the same within the error uncertainties involved (see Tables II and VIII). The level energy based on the two transitions to the ground and first excited states is  $1386.4 \pm 0.2$  keV from the  $(n, \gamma)$  measurement and  $1386.5 \pm 0.3$  keV from the  $\beta$ -decay measurement, respectively (see Tables VI and VII).

We have made an assignment of  $J^\pi = 2^+$  and note that a  $2^+$  assignment has been suggested from the Coulomb excitation work of Milner *et al.*<sup>17</sup> and from the  $\beta$ -decay work of Kukoc *et al.*<sup>4</sup> The latter points out that negative parity is not ruled out by their  $\gamma$ -ray data but is at variance with their  $\log ft$  value of 9.1.

Level at  $1431.3 \pm 0.3$  keV:  $J^\pi = 1^+, 2^+$

A primary  $E1$  transition following average resonance capture is observed having an intensity which may correspond to either of the two  $E1$  intensity groups. This limits the choices of spin and parity assignment to  $0^+$ ,  $1^+$ , or  $2^+$ . The energy is based on the 1431.5 and 1319.8 keV transitions. The ground state transition suggests that the  $0^+$  is a less likely choice. We have observed a weak 1450.5 keV transition in the  $\beta$ -decay spectrum (see Table II). Level energy values from high energy and medium energy  $(n, \gamma)$  data agree within errors [1431.2 keV  $(\bar{n}, \gamma)$  primary, 1431.1 keV  $(n, \gamma)$  primary, and 1431.3 keV  $(n, \gamma)$  medium energy]. This is consistent with the inelastic deuteron scattering measurements made by Günther *et al.*<sup>17</sup> that suggest either a  $0^+$  or  $2^+$  assignment for a level at 1432 keV.

The rest of the level scheme (Fig. 9) is based on  $(n, \gamma)$  data only, since the  $7^-$  state at  $1501.1 \pm 0.8$  keV (Fig. 3) is the highest energy state observed from the <sup>184</sup>Re  $\beta$ -decay data.

With the exception of two primary transitions shown plotted as solid squares in Fig. 7 (the  $6025.2 \pm 0.2$  keV transition to the 1386 keV level and the  $5603.5 \pm 0.4$  keV transition to the 1808 keV level), the positive parity states are well separated in intensity from the negative parity group. This allows one to give a definite positive parity and low spin assignment to 19 states above the 1501 keV level.

The positive parity state having spin 1 or 2 as reported by Casten and Kane<sup>16</sup> at 1570.6 keV using neutron capture in the 7.6 eV resonance is not observed in this work. If one applies the 30% error on the intensity which Casten and Kane<sup>16</sup> suggest for the primary  $\gamma$  transition to this state, it becomes equal to the weakest  $\gamma$  transition that they report (a transition to a level which they have stated is not definitely established). Though it is quite possible for the average resonance neutron capture spectrum to miss some low spin negative parity states, it is highly unlikely for it to miss a low spin ( $J = 0, 1, \text{ or } 2$ ) positive parity state. The recent 2 keV neutron capture studies by Greenwood and Reich<sup>11</sup> also fail to observe this state.

Levels at  $1613.2 \pm 0.6$  keV and  $1614.8 \pm 0.2$  keV

The average resonance neutron capture spectrum contains a line which is definitely a doublet with the stronger member of lower energy. We have fitted combinations of two  $E1$  transitions and combinations of an  $E1$  transition (lower energy member) with an  $M1$  transition to the doublet line shape, taking care to use the proper line shapes for each multipolarity. This process has ruled out any likelihood of two equal intensity  $\gamma$  transitions and has shown that the higher energy member must be less intense than the lower energy member by at least the 5:3 ratio predicted for  $1^+$  to  $0^+$  or  $2^+$  intensity ratios. Though the envelope can be fitted well enough by an  $E1 + M1$  pair of lines that negative parity cannot be entirely ruled out for the lower energy state, it is clear that a pair of  $E1$  transitions gives a somewhat better fit. If the level separation is held to that predicted by the secondary transitions from these states (1.6 keV), the fit with two  $E1$  transitions is clearly superior and best for a ratio of about 2:1.

These analyses suggest  $J^\pi$  assignments  $0^+$  or  $2^+$  for the 1613.2 keV state and  $1^+$  for the 1614.8 keV state. Greenwood and Reich<sup>11</sup> report two positive parity states at these energies but a spin of 1 and 0, respectively. Their 2 keV neutron capture spectrum apparently does not reveal the doublet

structure but they conclude that the 1614 keV state must be a double to account for the poor agreement between their energies deduced from primary transitions as compared to those deduced from the proposed secondary transitions.

Casten and Kane<sup>16</sup> have also reported a state at 1615 keV having positive parity and a spin of 1, though possibly 0 or 2. Several earlier resonance neutron capture experiments (Alves *et al.*<sup>10</sup> and Samour *et al.*<sup>15</sup>) led to a  $1^+$  assignment for a state at this energy.

The state at 1714 keV which is reported but not given a  $J^\pi$  assignment by Casten and Kane<sup>16</sup> has been reported as a  $1^+$  state by Beer *et al.*<sup>9</sup> based on a strong transition in the  $0^-$  resonance at 101 eV. Greenwood and Reich<sup>11</sup> have adopted the  $1^+$  assignment due to this earlier work although their 2 keV neutron capture data (see Fig. 3 and Table 2 of Ref. 11) places the intensity of the primary to this state among the weaker of the  $E1$  transitions. It appears that their 2 keV neutron-capture data does not separate the two  $E1$  intensity groups to the extent that our average capture process does but we would need to obtain better averaging if we were to rule out the  $1^+$  assignment, since we do have Porter-Thomas fluctuations showing up in the known  $2^+$  states. However, the assignment for this state which is consistent with our data is  $0^+$  or  $2^+$ , since it clearly falls into the lower intensity group of  $E1$  transitions (see Fig. 7).

We have given a tentative  $1^-$  assignment to the 1808 keV level and a  $2^+$  to the 1877 keV level. The former assignment is in disagreement with Greenwood and Reich<sup>11</sup> who have made a  $2^+$  assignment based on their 2 keV neutron-capture data. Reference to Fig. 3 in their paper indicates that these same two states are among three states having the lowest intensities of his positive parity group. The lowest intensity state of the three negative parity states shown in their Fig. 3 is the  $2^-$  state at 1131.2 keV (Ref. 11's value). Their  $0^+$  at 2126.6 keV is not well separated from this negative parity group as it is in our data, where it clearly falls within errors on the lower  $E1$  intensity line (see Fig. 7). Our  $(\bar{n}, \gamma)$  data has revealed 8, and possibly 11, negative parity states belong to  $^{184}\text{W}$ , excluding the 1808 keV case. Casten and Kane<sup>16</sup> have not ruled out positive parity, though they suggest a preference for negative parity for a state at 1809.5 keV having spin 0, 1, 2, or 3. Samour *et al.*<sup>15</sup> have reported an 1803 keV state with  $J^\pi = 0^+, 1^+, \text{ or } 2^+$ .

For the next five states there is agreement between our results and those reported by Greenwood and Reich<sup>11</sup> on energy and parity but we remove the  $J=1$  choice from the two states at 2013.2 and 2031.0 keV, while preferring it for the state at

1996 keV due to a possible ground state transition.

The  $1^-$  state at 2056.5 keV is a new level supported by an average capture primary, a thermal capture primary, and two depopulating transitions.

Our assignment of  $J^\pi = 0^+$  or  $2^+$  at 2062.8 keV agrees with Greenwood and Reich,<sup>11</sup> who include the  $J=1$  choice as well. Casten and Kane<sup>16</sup> have assigned a  $2^+$  to this state, while Samour *et al.* have assigned a  $1^+$ .

The  $0^-$  or  $2^-$  states at 2074.0 and 2084.8 keV are new levels, but are dashed in the level scheme since the only evidence for them are average capture primary transitions whose isotopic identification is most probably  $^{184}\text{W}$ , though this is not as firmly established as for other cases. Casten and Hansen<sup>21</sup> report a state at 2072 keV and suggest that it may correspond to the 2062 keV state, but that the energy disagreement makes for a doubtful identification.

The state at 2090.0 keV is supported by both thermal and average capture primary transitions but in each case it is known that there is a fraction of the line intensity due to interference from capture in  $^{186}\text{W}$ . Our  $1^-$  assignment is tentative and disagrees with the  $1^+$  assignment made by Samour *et al.*,<sup>15</sup> who may have been observing the next state at 2098.0 keV which we show as a  $1^+$  state, in agreement with Greenwood and Reich.<sup>11</sup>

We have observed two positive parity states at 2104.8 keV ( $J=1$  or 2) and 2111.2 keV ( $J=2$ ) (see Table VII and Fig. 9), in essential agreement with Greenwood and Reich.<sup>11</sup> They have reported a 982.44 keV  $\gamma$  ray and placed it as a possible transition from both of these states (their level values are 2104.2,  $J^\pi = 0^+, 1^+, 2^+$  and 2112.5 keV,  $J^\pi = 0^+, 1^+, 2^+$ , respectively). We have observed a singlet line at 980.5 keV having a relative intensity of 3.4 (see Table VIII). The ratio of its intensity in the enriched target spectrum to that from the natural abundance target spectrum is 20 times smaller than necessary for it to be a  $^{184}\text{W}$  line. However, the natural abundance target gives a very close doublet at 981.2 keV, the higher energy member of which belongs to an isotope other than  $^{184}\text{W}$ . It is most likely though not definite that the 980.5 keV  $\gamma$  ray is due to  $^{184}\text{W}$ . This  $\gamma$  ray could be a transition from the 2111 keV state to the 1130.4 keV state. The  $(\bar{n}, \gamma)$  primary  $\gamma$  transition intensity suggests a  $0^+$  or  $2^+$  assignment for the 2111 keV state and if the above transition is correct the  $2^+$  would be preferable. The 1099.5 keV transition from the 2104.8 keV state to the  $3^+$  state at 1005.9 keV suggests that  $J=0$  is least likely of the choices (0, 1, or 2) allowed by the average capture data.

We failed to detect the positive parity states at 2130 and 2145 keV reported by Samour *et al.*<sup>15</sup> and

also the  $0^+$  state at 2182 keV reported by Casten *et al.*<sup>21</sup> Our results suggest that the level at 2222.7 keV should have  $J^\pi = 0^+$  or  $2^+$  in agreement with Casten and Kane<sup>16</sup> and Casten *et al.*<sup>21</sup>

The 2246.4 keV state recently reported by Greenwood and Reich<sup>11</sup> as a positive parity state with a tentative spin assignment of 1 is observed in our average capture data. It has been reported by Samour *et al.*,<sup>15</sup> who assigned  $J^\pi = 2^+$  at 2250 keV, and by Stecher-Rasmussen *et al.*,<sup>30</sup> who assign spin 1 or 2 with a preference for 2. In our average capture spectrum the line corresponding to this state has the intensity of the weaker  $E1$  group, suggesting a  $J^\pi$  assignment of  $0^+$  or  $2^+$  and an energy of 2246.6 keV. The isotopic identification in this case is complicated because the natural abundance target data to which it was compared shows a line that is most probably a tight doublet containing both a  $^{184}\text{W}$  line and a line from the  $^{182}\text{W}(n, \gamma)^{183}\text{W}$  reaction. By using the interspectra intensity ratio established for other  $^{183}\text{W}$  lines and  $^{184}\text{W}$  lines we deduced the fraction of line intensity due to  $^{184}\text{W}$  (see Tables VI and VII).

The state at 2321.4 keV ( $J^\pi = 0^-, 2^-$ ) is a new level supported by thermal and average capture primary transitions but dashed in the level scheme since in the latter case the isotopic identification is not certain. One other state at 2352.6 keV is also given by Greenwood and Reich,<sup>11</sup> but they assign positive rather than negative parity. As can be seen from Fig. 7, this state separates nicely from the positive parity group into the stronger part of the negative parity group. The state at 2390.8 keV ( $J^\pi = 1^+$ ) is probably the same state reported by Yates *et al.*<sup>7</sup> but they made no  $J^\pi$  assignment.

The last state shown in Fig. 9, at 2404.2 keV with  $J^\pi = 0^+$  or  $2^+$ , is another new level. The evidence for this state is a strong  $E1$  average capture primary, a thermal capture primary, and a possible transition (1500.8 keV) to the  $2^+$  state at 903 keV.

#### SUMMARY

Except for the states at 1005.9 keV ( $3^+, 4^+$ ), 1133.6 keV ( $4^+$ ), and 364.1 keV ( $4^+$ ), the fact is that no spins higher than 2 are suggested for the

level scheme (Fig. 9) by the results of the various neutron capture  $\gamma$ -ray methods. In addition, almost all observed secondary transitions can be fitted into the level scheme. These facts suggest that states having spins 2 or more units higher than the higher capture state spin ( $J=1$ ) are not being fed with sufficient intensity to be observed in the cascading processes in this experiment. Thus there is very little chance to observe bands other than the ground state band. However, the fact that the data contain evidence for spins up to 2 units simplifies the level scheme and makes it possible for us to conclude that we have very likely found all the low spin (0, 1, and 2) positive parity states and a significant number of the low spin negative parity states.

We expect that the remaining unresolved questions and assignment choices for this partial level scheme can be answered by employing a bent crystal spectrometer to measure  $\gamma$ -ray energies below 600 keV. This perhaps would aid in locating states having higher spin values.

The likelihood is very small for having Porter-Thomas fluctuations large enough to suppress an average capture primary  $\gamma$  transition going to a positive parity low spin state so as not to be observed. We therefore should observe all such states unless their primary  $\gamma$  transitions are overlooked in close doublet or multiplet structures or their isotopic identity cannot be established. This suggests that the positive parity states at 1570.6 keV ( $1^+, 2^+$ ) (reported by Casten and Kane<sup>16</sup>) and 2182 keV ( $0^+$ ) (reported by Casten *et al.*<sup>21</sup>) may have higher spins or negative parity.

#### ACKNOWLEDGMENTS

Credits belong to a number of people at Argonne National Laboratory for making possible the effective use of the neutron capture  $\gamma$ -ray facilities. The authors wish to thank Dr. L. M. Bollinger for his assistance in initiating this project, Dr. G. E. Thomas for expert assistance and advice while conducting the experiments, and Mr. James Spect for invaluable technical services. Finally, we thank Mr. Harold Giddings of Northern Illinois University for valuable servicing of electronic equipment.

<sup>1</sup>N. R. Johnson, *Phys. Rev.* **129**, 1737 (1963).

<sup>2</sup>B. Harmatz and T. H. Handley, *Nucl. Phys.* **56**, 1 (1964).

<sup>3</sup>J. Glatz, K. Lobner, and F. Opperman, *Z. Phys.* **227**, 83 (1969).

<sup>4</sup>A. Kukoc, B. Singh, J. King, and H. Taylor, *Nucl. Phys.* **A143**, 545 (1969).

<sup>5</sup>S. E. Bodenstedt, E. Mathias, H. J. K rner, E. Gerden,

F. Frisius, and D. Hovestadt, *Nucl. Phys.* **15**, 239 (1960).

<sup>6</sup>M. J. Canty, C. G nther, P. Herzog, and B. Richter, *Nucl. Phys.* **A203**, 421 (1973).

<sup>7</sup>S. W. Yates, P. J. Daly, N. R. Johnson, and N. K. Aras, *Nucl. Phys.* **A204**, 33 (1973).

<sup>8</sup>D. J. McMillan, R. C. Greenwood, C. W. Reich, and

- R. G. Helmer, Nucl. Phys. A223, 29 (1974).
- <sup>9</sup>M. Beer, M. Bhat, R. Chrien, M. Lone, and O. Wasson, in Proceedings of the Conference on Slow Neutron-Capture Gamma-Ray Spectroscopy, 1960 (unpublished), p. 459 (ANL Report No. ANL-7282).
- <sup>10</sup>R. N. Alves, C. Samour, J. M. Kuchly, J. Julien, and J. Morgenstern, National Bureau of Standards Special Publication No. 299, Vol. 2, 783 (1968).
- <sup>11</sup>R. C. Greenwood and C. E. Reich, Nucl. Phys. A223, 66 (1974).
- <sup>12</sup>R. R. Spencer and K. T. Faler, Phys. Rev. 155, 1368 (1967).
- <sup>13</sup>K. T. Faler, R. R. Spencer, and R. A. Harlan, Phys. Rev. 175, 1495 (1968).
- <sup>14</sup>E. R. Rae, W. R. Moyer, R. R. Fullwood, and J. L. Andrews, Phys. Rev. 155, 1301 (1967).
- <sup>15</sup>C. Samour, J. Julien, R. N. Alves, S. deBarros, and J. Morgenstern, Nucl. Phys. A123, 581 (1969).
- <sup>16</sup>R. F. Casten and W. R. Kane, Phys. Rev. C 7, 419 (1973).
- <sup>17</sup>C. Günther, P. Keinheinz, R. F. Casten, and B. Elbek, Nucl. Phys. A172, 273 (1971).
- <sup>18</sup>W. T. Milner, F. K. McGowan, R. L. Robinson, P. H. Stelson, and R. O. Sayer, Nucl. Phys. A177, 1 (1971).
- <sup>19</sup>R. G. Stokstad and B. Persson, Phys. Rev. 170, 1072 (1968).
- <sup>20</sup>P. Kleinheinz, P. J. Daly, and R. F. Casten, Nucl. Phys. A208, 93 (1973).
- <sup>21</sup>R. F. Casten and O. Hansen, Nucl. Phys. A210, 489 (1973).
- <sup>22</sup>T. Butz, G. Eska, E. Hagen, and P. Kienle, Z. Physik, 254, 312 (1972).
- <sup>23</sup>H. Hubel and C. Günther, Nucl. Phys. A210, 317 (1973).
- <sup>24</sup>K. S. Krane, C. E. Olsen, and W. A. Steyert, Phys. Rev. C 7, 263 (1973).
- <sup>25</sup>L. M. Bollinger and G. E. Thomas, Phys. Rev. C 2, 1951 (1970).
- <sup>26</sup>G. E. Thomas, D. E. Blatchley, and L. M. Bollinger, Nucl. Instrum. Methods 56, 325 (1967).
- <sup>27</sup>G. E. Thomas, private communication.
- <sup>28</sup>M. G. Strauss, F. R. Lenkszus, and J. J. Eickholz, Nucl. Instrum. Methods 76, 285 (1969) [ANL Report No. ANL-7282, 1966 (unpublished), p. 113].
- <sup>29</sup>L. M. Bollinger, R. E. Coté, R. T. Carpenter, and J. P. Marion, Phys. Rev. 132, 1640 (1963).
- <sup>30</sup>F. Stecher-Rasmussen, J. Kopecky, K. Abrahams, and W. Ratynski, Nucl. Phys. A181, 250 (1972).